SEMMELWEIS EGYETEM

DOKTORI ISKOLA

Ph.D. értekezések

3135.

HORVÁTHNÉ NÉMETH ZSUZSANNA

Vaszkuláris patofiziológia / atherosclerosis

című program

Programvezető: Dr. Prohászka Zoltán, egyetemi tanár
Témavezető: Dr. Cervenak László, tudományos főmunkatárs

COOPERATIVE EFFECTS OF MASP-1 AND OTHER ACTIVATING SIGNALS ON ENDOTHELIAL CELL BEHAVIOR

PhD thesis

Zsuzsanna Horváthné Németh

Theoretical and Translational Medicine Doctoral School

Semmelweis University

Supervisor:	László Cervenak, Ph.D
Official reviewers:	Tamás Mihály Cserepes, Ph.D
	Krisztina Futosi, Ph.D

Head of the Complex Examination Committee: György Reusz, MD, D.Sc

Members of the Complex Examination Committee: Ákos Jobbágy, DSc

Tamás Radovits, MD, Ph.D

Budapest

2024

TABLE OF CONTENTS

LIST OF ABBREVIATIONS

BCEN	bovine corneal endothelial cell
bFGF	basic fibroblast growth factor
B2R	bradykinin receptor B2
CBP	CREB binding protein
CREB	cAMP response element binding protein
DAMPs	damage-associated molecular patterns
ECs	endothelial cells
EDHF	endothelium derived hyperpolarizing factor
ET-1	endothelin-1
GPCR	G protein coupled receptor
GSEA	gene set enrichment analysis
HAE	hereditary angioedema
HMWK	high molecular weight kininogen
HUVEC	human umbilical vein endothelial cell
ICAM-1	intercellular adhesion molecule 1
IFNγ	interferon γ
IFNGR	interferon gamma receptor
Il-1β	interleukin 1β
IL-6	interleukin 6
IL-8	interleukin 8
iNOS	inducible nitric oxide synthase
LPS	lipopolysaccharide
MASP-1	mannan-binding lectin-associated serine protease-1
MBL	mannose-binding lectin
MDCK	Madin-Darby canine kidney cell
MHC	major histocompatibility complex
MLC	myosin light chain
NF-κB	nuclear factor kappa B
NES	normalized enrichment scores
NO	nitric oxide
PAMPs	pathogen associated molecular patterns
PAR	protease activated receptor

3

PRMs   pattern recognition molecules

qPCR   quantitative real-time PCR

ROCK   Rho-associated coiled-coil kinase

TAFI   thrombin-activatable fibrinolysis inhibitor

TF   tissue factor

VCAM-1   vascular cell adhesion molecule 1

1. INTRODUCTION

1.1 Endothelial cells

Endothelial cells (ECs) create the innermost layer of the vessel walls, forming an interface between circulating blood and the surrounding tissue. ECs, due to their locations, are directly affected by the soluble molecules and cells in the blood plasma, therefore they act as signal integrators. The endothelium plays a role in a large number of physiological and pathological processes (**Figure 1**) (1).
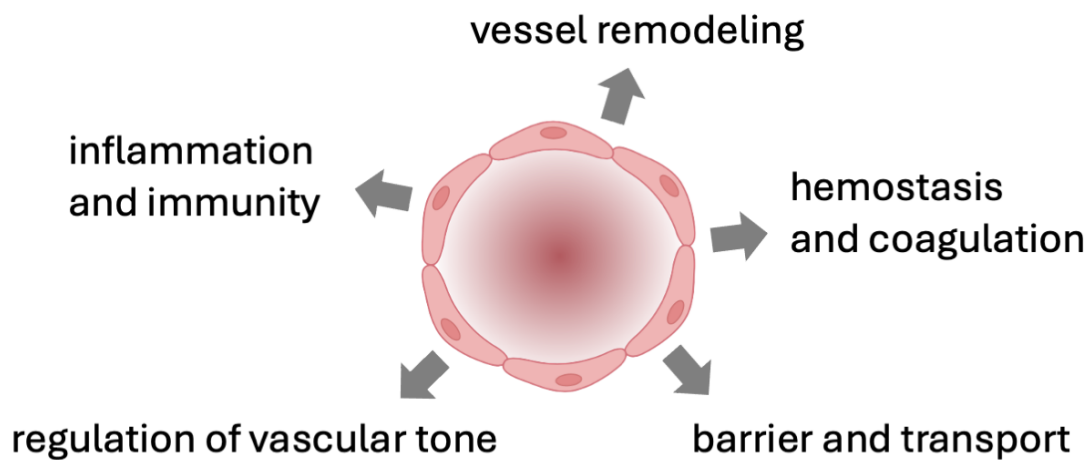
Figure 1. Schematic representation of the main endothelial cell functions.

ECs maintain homeostasis by keeping blood in a fluid state and promote limited clot formation when the integrity of the vascular wall is compromised. The endothelium is semipermeable, it allows the regulated transport of solutes and fluids into and out of the blood, primarily in the capillaries. Another important process is leukocyte trafficking, a multistep adhesion cascade taking place mostly in the postcapillary venules, ensuring the migration of immune cells into the tissues through the paracellular and transcellular route (2). ECs contribute to the control of vascular tone by releasing vasoactive factors. These can be involved in vasodilation such as nitric oxide (NO), prostacyclin and endothelium derived hyperpolarizing factor (EDHF) or in vasoconstriction like thromboxane and endothelin-1 (ET-1) (3). Maintaining and restoring the integrity of the circulatory system has a fundamental importance. Angiogenesis is the process of vascular growth by sprouting of existing vessels during embryonic development, growth, regeneration, and wound healing (4). The endothelium also significantly contributes to the processes of both innate and adaptive immunity. ECs have many immune functions including cytokine

secretion, phagocytosis, antigen presentation, sensing of pathogen- and damage associated molecular patterns (PAMPs and DAMPs, respectively), immunosuppression and the enhancement of pro-inflammatory or anti-inflammatory response (5).
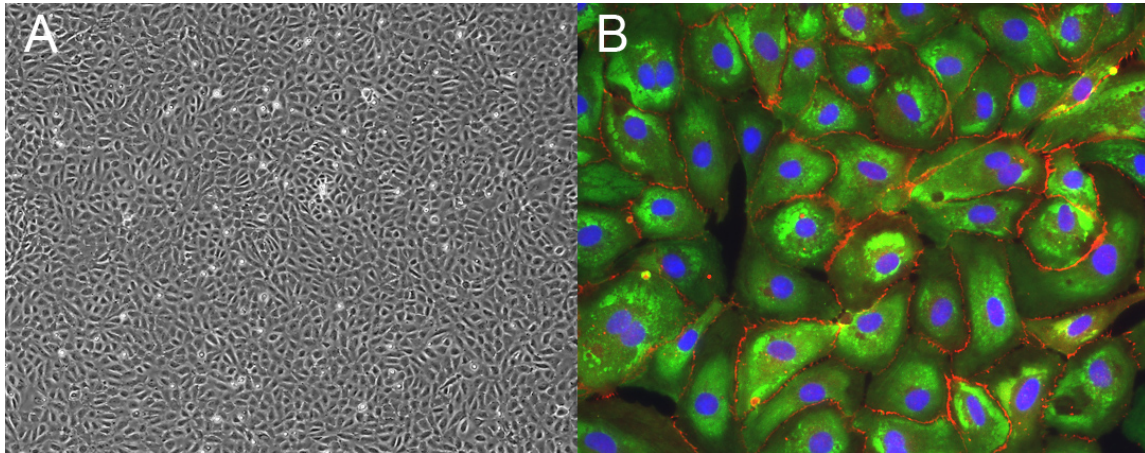
Figure 2. Microscopic pictures of human umbilical vein endothelial cells (HUVECs). Using phase contrast microscopy typical cobblestone morphology is visible (A). ECs express VE-cadherin (red) and PECAM-1 (green) adhesion molecules. Blue: nuclear staining. The candidate's own photos.

1.2 MASP-1

Mannan-binding lectin associated serine protease-1 (MASP-1) is one of the key components of the complement lectin pathway (**Figure 3**). Mannan-binding lectin (MBL), collectin-10 and -11 and the ficolins (ficolin-1,2,3) are the soluble pattern recognition molecules (PRMs) of the complement lectin pathway and they circulate in the blood in complexes with associated serine proteases (MASP-1 and -2). They recognize and bind to pathogens (PAMPs) and altered host cells (DAMPs). The recognition leads to the autoactivation of MASP-1, which activates MASP-2, initiating the complement lectin pathway by generating C3 convertase (6).
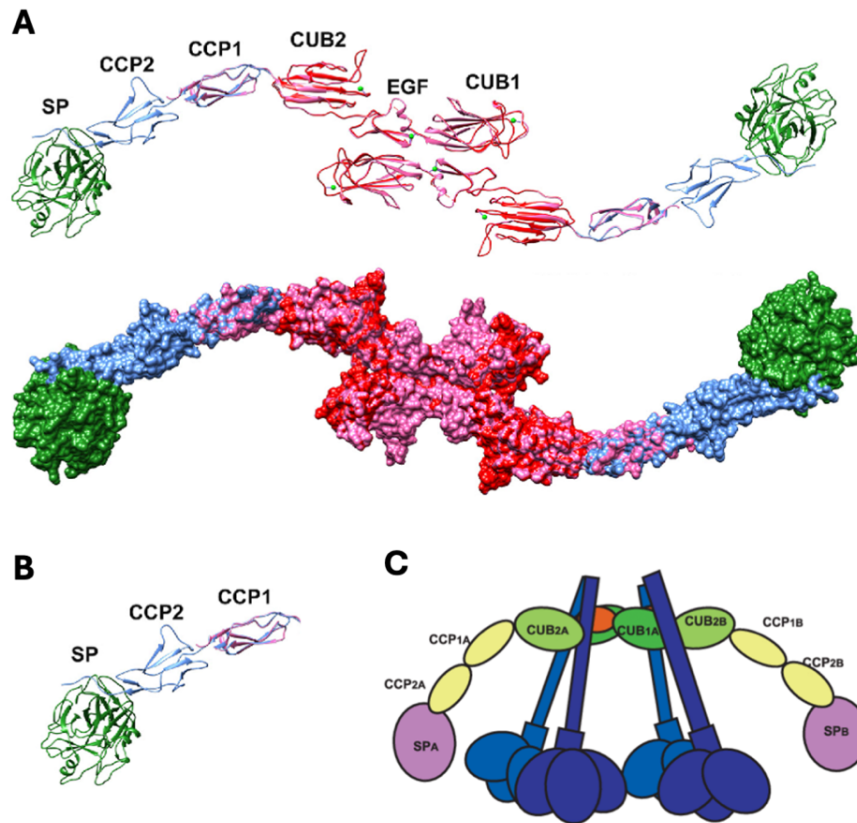
Figure 3. *(A) Structural model of a MASP-1 dimer (7) (B) Structural model of the recombinant MASP-1 (rMASP-1) (C) Schematic model of an MBL complex. MBL is shown in blue (8).*

Besides, being a promiscuous protease with a relatively large and open substrate-binding site, MASP-1 is able to cleave a great variety of substrates (**Figure 4**) (9). It cleaves fibrinogen, factor XIII, thrombin-activatable fibrinolysis inhibitor (TAFI) and prothrombin, promoting blood clotting and coagulation (10-13). Furthermore, MASP-1 is able to deliberate bradykinin from high molecular weight kininogen (HMWK) (14). Moreover, as we have shown previously, MASP-1 is able to activate endothelial cells by the cleavage of protease-activated receptors (PARs), namely PAR-1, 2 and 4 (15). This activation induces ECs to acquire a pro-inflammatory phenotype characterized by the activation of pro-inflammatory genes (16), expression of IL-6 and IL-8 pro-inflammatory cytokines (17), induction of E-selectin expression, enhanced adhesion between ECs and neutrophils (18) and increased permeability (19). Furthermore, MASP-1 can synergize with other pro-inflammatory activators to enhance the inflammatory response (20) and its effect is potentiated by hypoxia on ECs (21).
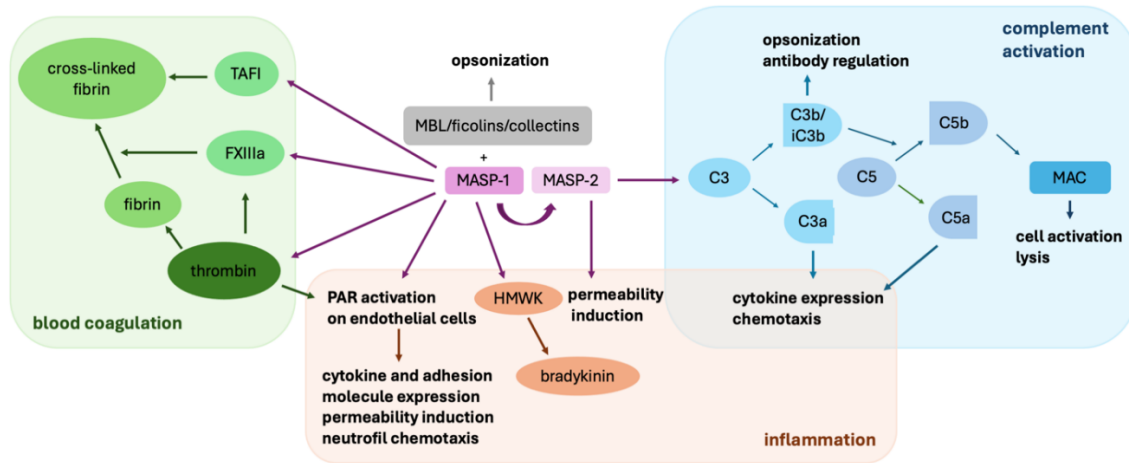
Figure 4. MASP-1 has diverse functions, it not only initiates the activation of complement lectin pathway but also modulates inflammation and blood coagulation (9-19).

1.3 Inflammatory mediators

A great variety of substances from diverse sources can activate endothelial cells to acquire a proinflammatory phenotype.

Bacterial lipopolysaccharide (LPS) is the major structural component of the outer wall of Gram-negative bacteria, which triggers severe inflammatory reactions in the human body via the LBP/CD14/TLR4/MD2 receptor complex (22). The receptor complex activation leads to MyD88-dependent early nuclear factor kappa B (NF-κB) activation and MyD88-independent late NF-κB activation (23). Besides, the p38 MAPK, JNK and Akt signaling pathways are also activated (24). LPS is a potent activator of endothelial cells causing extensive expression of inflammatory cytokines (IL-6, IL-8 and IL-1β), adhesion molecules (E-selectin, ICAM-1 and VCAM-1) and induces apoptosis (25). LPS plays a pivotal role in the pathogenesis of sepsis and even with the recent advances in therapies and overall medical care, Gram-negative bacterial sepsis is still a common life-threatening event.

Bradykinin is a small oligopeptide liberated from high molecular weight kininogen (HMWK) by plasma serine proteases (mainly plasma kallikrein and to a lesser extent, other enzymes, including MASP-1 (14)) and acts predominantly on bradykinin receptor B2 (B2R). Bradykinin is a potent vasodilator, increases endothelial permeability, and increases endothelial nitric oxide (NO) production (26-29).
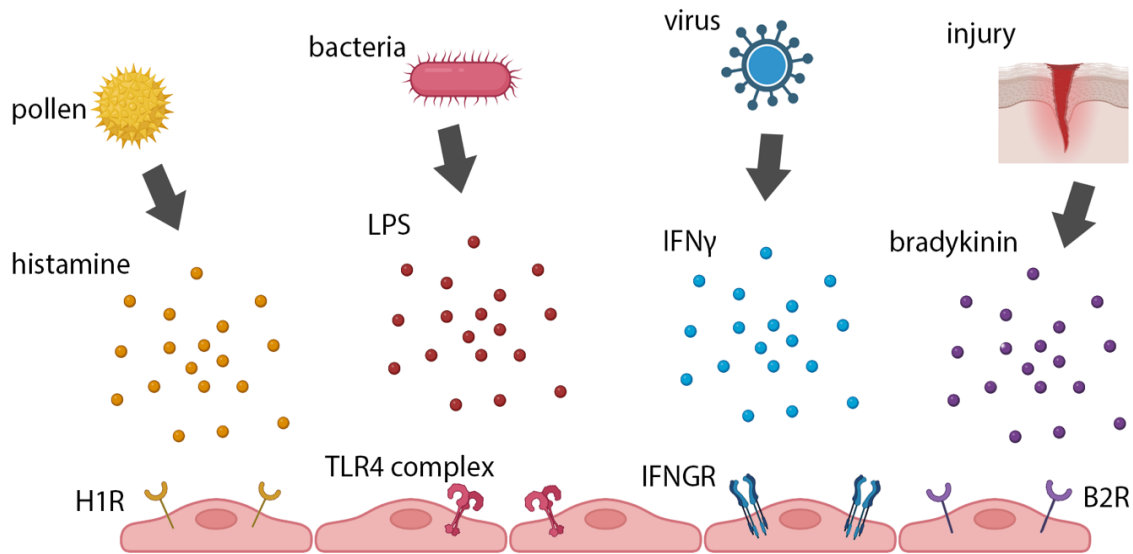
Figure 5. *Different stimuli promote the liberation of variety of mediators which results in the activation of endothelial cells via different receptors on the surface of the endothelium.*

Histamine is the major mediator of acute allergic reactions, released mostly from basophil granulocytes and mast cells, and acts on four (H1R-H4R) receptors. One of its major effects in the vascular system is the induction of NO production through H1R activation, which leads to the dilation of blood vessels (30, 31).

During viral infections, IFNγ is produced predominantly by T_H1, T_C1 and NK cells. Its receptor (IFNGR) enhances antigen presentation, increases the expression of major histocompatibility complex (MHC), activates the inducible nitric oxide synthase (iNOS), promotes adhesion and leukocyte migration, and increases endothelial permeability (32).

1.4 Wound healing

Wound healing begins at the moment of injury and normally advances through the sequential stages of hemostasis, inflammatory response, proliferative phase, and remodeling phase. It is a complex event, where several cell types interact with various functions (**Figure 6**). The earliest responses to injury are designed to prevent blood loss, through the activation of a cascade of serine proteases, which result in platelet activation and fibrin clot formation. Besides preventing bleeding, it is also a supportive matrix for invading cells that are needed at the later stages. The inflammatory phase occurs during the first 72 hours after tissue injury. It consists of the release of inflammatory mediators, activation of the complement cascade and the facilitation of neutrophil and monocyte

infiltration. At the site of an acute injury, damage-associated molecular patterns (DAMPs) and – if the wound is contaminated by pathogens – pathogen-associated molecular patterns (PAMPs) appear, which leads to local cell activation and the propagation of the inflammatory response. During the normal process of wound healing M2 type, anti-inflammatory macrophages and regulatory T cells are responsible for the tempering down of inflammation. After the inflammation resolved, the proliferation phase begins. It involves the restoration of the vascular network (angiogenesis), formation of granulation tissue and reepithelization. Finally, weeks after wounding, the remodeling phase starts. With the slowing of angiogenesis and replacing type III collagen with a stronger type I collagen, the granulation tissue transforms into a scar. The process is mainly driven by myofibroblasts. Recently it has been shown that the key transition point in wound healing is between the inflammatory and proliferative phases. If the inflammation does not subside, a non-healing (chronic) wound develops (33).

Time from injury	seconds to hours	hours to days	days to weeks	weeks to months
	Hemostasis phase	Inflammatory phase	Proliferative phase	Remodeling phase
Participants	platelets complement kinins	platelets neutrophils macrophages endothelial cells	macrophages lymphocytes fibroblasts epithelial cells endothelial cells	fibroblasts epithelial cells
Major events	coagulation vasoconstriction	phagocytosis and removal of pathogens by neutrophils (earlier), macrophages and T cells (later)	fibroblast proliferation collagen synthesis angiogenesis reepithelization granulation tissue formation	remodeling reepithelization scar tissue formation
Functions of endothelial cells	hemostasis regulation	increased permeability expression of cytokines and adhesion molecules	angiogenesis	decreased blood flow and number of vessels

Figure 6. *Phases of the normal wound healing process and the corresponding time scale.*

1.4.1 Endothelial cells during wound healing

Endothelial cells actively participate in wound healing processes. Normally, they promote anti-coagulant properties and counteract platelet activation, however, if activated by vasoactive agents they release von Willebrand factor (VWF), PAR receptors, thromboxane and plasminogen-activator-inhibitor 1 (PAI-1) that promotes the binding of platelets (34). Furthermore, vasoconstriction is an important initial response in the case of vessel damage. It is caused by direct access of smooth muscle cells to locally generated vasoactive agents and by bypassing the vasodilatory action of ECs (35).

During the inflammatory phase, increased endothelial permeability and increased expression of adhesion molecules promote the transmigration of immune cells. ECs also participate in the chemotaxis of neutrophil granulocytes by the expression of various cytokines and chemokines (17, 36).

In the granulation phase, angiogenesis is initiated by a diverse group of growth factors. Endothelial cells undergo a series of morphological alterations and chemotactic agents direct the cell movement throughout the process (37). They migrate at the fastest pace immediately after injury, then enter a slower migration rate that they maintain during the healing process (38). Capillary sprouts from the wound edge invade the blood clot and form a new microvascular network within a few days. The transient fibrin matrix is an excellent matrix for ECs to act as a scaffold for new capillary structures (39). With time the fibrin-based provisional matrix is replaced by the acute granulation tissue (composed mainly by collagen, fibrinogen, fibronectin and hyaluronic acid). Gradually, collagen accumulates, the density of blood vessels decreases, and the granulation tissue turns into a scar. In the final remodeling phase, the blood flow decreases with the moderating metabolic activity of the scar (40).

1.5 NF-κB and CREB signaling pathways in endothelial cells

Although endothelial cells possess dozens of active signaling pathways mediating complex proinflammatory stimuli, two of them are worth to highlight due to their participation in many related processes from wound healing to proliferation and homing regulation. One of these key transcriptional factors is NF-κB, which is inhibited by IκB proteins (by masking the nuclear localization signal) in unstimulated ECs. Triggering of the canonical pathway (e.g. by TNFα, LPS or IL-1) cause the phosphorylation and ubiquitination of IκB proteins, which leads to their degradation. Alternatively, NF-κB can be activated by the noncanonical pathway, which is triggered by LPS, CD40, lymphotoxin and late membrane protein 1, among others. Finally, NF-κB enters the nucleus and induce the expression of a great variety of genes (41), and participates in proliferation/apoptosis balance as well as other processes related to inflammation and wound healing.

cAMP response element binding protein (CREB) is transcription factor that regulates diverse cellular responses, including proliferation, survival, and differentiation (42). It has also been shown to induce transcription of immune-related genes that possess a CRE element, including IL-2, IL-6, IL-10, TNFα, and cyclooxygenase-2 (43). Phosphorylation

of CREB (on Serine 133) is induced by cAMP or calcium (among others) leads to its interaction with its coactivator protein (CREB-binding protein (CBP) and its paralogue p300) to initiate transcription of CREB-responsive genes (44). It has been described that CREB phosphorylation inhibits NF-κB activation in endothelial cells by competing with it for the coactivator CBP (NF-κB interacts with CBP/p300 with the same region as phosphorylated CREB) (45, 46).

2. OBJECTIVES

As described earlier, endothelial cells act as important signal integrators, and MASP-1, the most abundant enzyme of the complement lectin pathway induces a proinflammatory phenotype in ECs. MASP-1 activation is triggered by different pathogens and altered host cells, and these stimuli not only activate the complement system, but also lead to the presence of various proinflammatory components in the blood (e.g. LPS, histamine, bradykinin, IFNγ), which can simultaneously alter endothelial cell behavior. The cellular response of ECs to injury is still a matter of active investigation and the participation of the lectin pathway in wound healing processes is actively researched in the context of atherosclerosis and atherosclerosis-related diseases (47, 48) as well as in the healing of chronic wounds (49). However, there is no data available about the effect of MASP-1 in the normal wound healing processes of otherwise healthy individuals.

Therefore, we established the following objectives for our research:

1. Does MASP-1 cooperate with other proinflammatory factors in endothelial cells in the induction of:
    a. Ca^{2+}-mobilization
    b. adhesion molecule expression
    c. cytokine expression
    d. permeability?

2. Does MASP-1 and other proinflammatory activators modifies each other's receptor expression at mRNA level?

3. How do endothelial cells response to mechanical wounding (signaling pathway activation, adhesion molecule expression)?

4. Does MASP-1 modify the speed of wound healing and the capillary network formation of endothelial cells?

5. Can we observe cooperation between MASP-1 and mechanical wounding in the induction of:
    a. Ca^{2+}-mobilization
    b. signaling pathways
    c. adhesion molecule expression?

3. METHODS

3.1 Reagents

The recombinant catalytic fragment of human MASP-1 (CCP1-CCP2-SP, hereinafter: rMASP-1) was expressed in *Escherichia coli* and purified by the method described by Dobó et al. (9). rMASP-1 preparations were free of bacterial contaminations and could be inhibited by C1-inhibitor as previously described (50, 51).

All other reagents were purchased from Merck-Sigma-Aldrich, unless otherwise stated.

3.2 Preparation and culturing of HUVECs

Endothelial cells were harvested from fresh umbilical cords obtained during delivery of healthy neonates by cesarean sections by collagenase digestion as described earlier (52). HUVECs were grown in gelatin-precoated flasks (Corning™ Costar™) in MCDB-131 medium (ThermoFisher Scientific) supplemented with 5% heat-inactivated calf serum (FCS), 2 ng/ml of human recombinant epidermal growth-factor (R&D Systems), 1 ng/ml of human recombinant basic fibroblast growth factor, 0.3% Insulin Transferrin Selenium (ThermoFisher Scientific), 1% Chemically Defined Lipid Concentrate (ThermoFisher Scientific), 1% Glutamax solution (ThermoFisher Scientific), 1% Penicillin-Streptomycin antibiotics solution, 5 µg/ml of Ascorbic acid, 250 nM of Hydrocortisone, 10 nM of HEPES, and 7.5 U/ml of heparin; hereinafter referred as Comp-MCDB. For some experiments, the medium was replaced with AIM-V medium (ThermoFisher Scientific) supplemented with 1% FCS, 2 ng/ml of human recombinant epidermal growth-factor (R&D Systems), 1 ng/ml of human recombinant basic fibroblast growth-factor, and 7.5 U/ml of Heparin; hereinafter referred as Comp-AIM-V.

Each experiment was performed in at least three independent, primary HUVEC cultures from different individuals, before passage 4. The study was conducted in conformity with the WMA Declaration of Helsinki; its protocol was approved by the Semmelweis University Institutional Review Board (permission number: TUKEB141/2015). All participants provided their written informed consent before inclusion.

3.3 Intracellular Ca^{2+}-mobilization assay

Intracellular Ca^{2+}-mobilization was measured using the method described previously (15). HUVECs were seeded in 96-well plates in 100% confluency and cultured in Comp-MCDB medium for 24 hours then the medium was changed to Comp-AIM-V for additional 24 hours.

Experiments in results 4.1:

The cells were pretreated with the selected agonist in predetermined suboptimal dose (rMASP-1: 0.6 μM, LPS: 10 ng/ml, histamine: 5 μM, IFNγ: 2 ng/ml or bradykinin: 2 μM) for 24 hours or were not pretreated. Suboptimal dose refers to the concentration of the selected activator where we could observe an approximately half-maximum response according to our previous experiments (17). 2 μM Fluo-4-AM (ThermoFisher Scientific) was used to load the cells for 20 minutes, then cells were incubated in HBSS for another 20 minutes. Measurements were carried out with fluorescence microscopy; sequential images were taken every 5 seconds. To determine baseline fluorescence, two images were taken before adding the treatment. Twenty cells per image were analyzed using CellP software (version 5.2), to calculate changes in fluorescence intensity. Images were background corrected and normalized to control.

Experiments in results 4.2

2 μM Fluo-4-AM (ThermoFisher Scientific) was used to load the cells for 20 min, then the cells were incubated in HBSS for another 20 min. When needed, apyrase (an ATP-diphosphatase) treatment (10 U/ml) was added to the cells for 5 minutes before the measurements. The measurements were carried out with fluorescence microscopy, the sequential images were obtained every 5 s. To determine the baseline fluorescence, two photos were taken before adding the treatment or scratching the cells. The scratching of the cell layer was carried out using a sterile needle. In some of the measurements 0.6 μM rMASP-1 was added to the wells 5, 10, 20 or 30 minutes after scratching. At least twenty cells were analyzed for each distance (100 μm, 200 μm, 300 μm and 400 μm) using the CellP software (version 5.2), to calculate changes in fluorescence intensity. Images were background corrected and normalized to control.

3.4. Adhesion molecule expression measured by cell-based ELISA

HUVECs were cultured in 96-well plates at 100% confluency in Comp-MCDB medium for 24 hours. They were then pretreated with the selected agonist at suboptimal doses or not pretreated. After 24-hour pretreatment, the cells were treated with agonists for E-selectin measurement for 6 hours or for VCAM-1 measurement for 24 hours. The cells were fixed and stained with mouse anti-human E-selectin (ThermoFisher Scientific) or mouse anti-human VCAM-1 (BD Biosciences) antibodies at room temperature for 1 hour. Then, HRP-conjugated goat anti-mouse antibody (Southern Biotech) and 3,3'5,5'-Tetra Methyl Benzidine were used to measure the expression of adhesion molecules.

3.5 Visualization of adhesion molecules by fluorescent microscopy

Confluent layers of endothelial cells were seeded and cultured for a day in 96 well plates in Comp-MCDB medium. The monolayer of cells was scratched 24, 6 or 2 hours before fixation. To some of the wells, 0.6 μM rMASP-1 treatment was added. The cells were fixed in ice-cold methanol-acetone (1:1) for 10 minutes. Then the cells were stained with primary anti-human antibodies (as indicated in **Table 1**) followed by Alexa568 conjugated goat anti-mouse IgG (1:500) and Hoechst 33342 (1:50000, Invitrogen). The images were taken with an Olympus IX-81 fluorescence microscope and an XM-10 camera.

Table 1. *Primary antibodies used for visualization of adhesion molecules.*

Antibody	Producer	Dilution
mouse anti-human E-selectin	Invitrogen	1:500
mouse anti-human ICAM-1	Invitrogen	1:500
mouse anti-human VCAM-1	BD Pharmingen	1:500

3.6 Measurement of IL-8 cytokine production by sandwich ELISA

HUVECs were seeded in 96-well plates at 100% confluency and cultured in Comp-MCDB medium for 24 hours. They were then pretreated with the selected agonist at suboptimal doses or not pretreated. After 24-hour pretreatment, the cells were treated with the agonists for 24 hours and the supernatants were collected. Supernatants were diluted in 1:20 and IL-8 was measured by sandwich ELISA kit (R&D Systems) according to the manufacturer's instructions.

3.7 Permeability measurement

Permeability tests were carried out using a modified version of the XPerT technique as described earlier (19). Briefly, HUVECs were seeded in 96-well plates pre-coated with biotinylated gelatin at 100% confluency and cultured in Comp-AIMV medium. After various pretreatments and treatments, Streptavidin-Alexa488 (ThermoFisher Scientific) was added to each well for 2 minutes. The cells were fixed with 1% paraformaldehyde-PBS and fluorescence plate reader (Tecan Infinite™ M1000 Pro) was used to quantify fluorescence. Representative images of each well were also taken using an Olympus IX-81 fluorescence microscope.

3.8 RNA purification and quantitative real-time PCR (qPCR)

HUVECs were cultured in 24-well plates to 100% confluency in Comp-MCDB medium, then treated with IFNγ (20 ng/ml), bradykinin (20 μM) or LPS (100 ng/ml) for 2 or 24 hours. RNA isolation was carried out using the illustra™ RNASpin RNA Isolation Kit (GE Healthcare) according to the manufacturer's protocol. RNA-cDNA transcription was performed with the Tetro cDNA Synthesis Kit (Bioline). SensiFAST SYBR Master Mix – No ROX Kit (Bioline) was used for quantification of cDNA using a Rotor-Gene Q (Qiagen) real-time PCR cycler. Primers (**Table 2**) were designed using the NCBI Primer-BLAST primer design tool and synthetized by IDT (Coralville, IA). The purity and size of PCR products were checked by sequencing (sequencing was performed by Biomi Ltd., Hungary) after the first use of each primer pair and by high resolution melting curve analysis for each measurement.

Quantification was performed using the Rotor-Gene Q Pure Detection 2.1.0 software (Qiagen), and values of interest were normalized with that of β-actin.

Table 2. Primers used in the qPCR reactions.

β-actin (ACTB)	forward	5'-ATCAAGATCATTGCTCCTCCTGA-3'
	reverse	5'-AAGGGTGTAACGCAACTAAGTCA-3'
B1 bradykinin receptor (BDKRB1)	forward	5'-CACAGAGTGCTGCCAACATTTAT-3'
	reverse	5'-ACTGGTTCCAGATATTCTCTGCC-3'
B2 bradykinin receptor (BDKRB2)	forward	5'-TCTGAGTCCAAATGTTCTCTCCC-3'
	reverse	5'-AGGACAAAGATGTTCTCTAGGGTG-3'
Histamine H1 receptor (HRH1)	forward	5'-GTCTTCATCCTGTGCATTGATCG-3'
	reverse	5'-AAGTCTGTCTCACACTTGTCCTC-3'
Proteinase-activated receptor 1 (F2R)	forward	5'-CTGTGTACACCGGAGTGTTTGT-3'
	reverse	5'-AGTAAAATGCTGCAGTGACGAA-3'
Proteinase-activated receptor 2 (F2RL1)	forward	5'-AAGAGGGCCATCAAACTCATT-3'
	reverse	5'-GTTCTTTGCATGATCCCTGAA-3'
Proteinase-activated receptor 4 (F2RL3)	forward	5'-ACCATGCTGCTGATGAACCT-3'
	reverse	5'-AGCACTGAGCCATACATGTGAC-3'

3.9 Measurement of CREB phosphorylation and NF-κB activation by fluorescent microscopy

HUVECs were seeded onto 96-well plates at 100% confluency and cultured for 2 days in Comp-MCDB medium. Apyrase treatment (10 U/ml) was added to some wells for 5 minutes prior to making the "wound". The monolayer of cells was scratched with a sterile pipette tip 10, 15, and 30 minutes (CREB phosphorylation) or 15, 30 and 60 minutes (NF-κB activation) before fixation. To some of the wells, 0.6 μM rMASP-1 treatment was added after scratching. The cells were fixed in ice-cold methanol-acetone (1:1) for 10

minutes. The cells were stained with rabbit anti-human phospho-CREB (1:200, Cell Signaling Technology Inc.) antibody or rabbit anti-human NF-κB p65 (1:200, Santa Cruz Biotechnology) antibody followed by Alexa568 conjugated goat anti-rabbit IgG (1:500) and Hoechst 33342 (1:50000, Invitrogen). The photos were taken using an Olympus IX-81 fluorescence microscope. All analyses were performed using the original, unmodified images with CellP software (version 5.2).

3.10 Wound healing assay

Confluent layers of endothelial cells were seeded and cultured for 2 days in 96 well plates in Comp-MCDB medium. The wound was made manually by scratching the monolayer of the cells with a sterile pipette tip. Then basic fibroblast growth factor (bFGF) (1.6 ng/ml) or rMASP-1 (2 μM) treatment was added. Photos were taken after 0, 2, 4, 6, 24, 30 and 48 hours on a microscope with a relative objective of 20x. Analysis of the area of the remaining wound in each image was performed using ImageJ software (version 1.54e).

3.11 Capillary network integrity - Matrigel assay

HUVECs were seeded onto ibidi Angiogenesis plates in 100% confluency and cultured for 16 hours until typical network-like structures were formed in Comp-MCDB medium. 2 μM rMASP-1 treatment was added to the cells. The wells were photographed 0, 2, 3, 6, 8, 12, 24, 30 and 48 hours after the treatment. The number of branching points were measured using Image J software (version 1.54e) (53).

3.12 Statistical analysis

Experiments were performed in analytical duplicates (for Ca^{2+}-mobilization assay, phospho-CREB and NF-κB activation measurement, adhesion molecule visualization and mRNA measurement) or triplicates (for cell-based ELISA, cytokine ELISA, wound healing assay, Matrigel assay and permeability measurements) and repeated at least three times using HUVECs from different individuals. Statistical analysis was performed after evaluating normality using Student's t-test, one-sample t-test, one-way ANOVA or two-way ANOVA with GraphPad Prism 10. software (GraphPad). A $p \leq 0.05$ was considered statistically significant. Data are presented as means ± SEM unless otherwise stated.

3.12.1 Gene set enrichment analysis (GSEA)

We used the same microarray database that we described in our previous article (16), classical GSEA analysis was performed using GSEA version 4.3.2 from the Broad Institute (MIT) (54). Normalized Enrichment Scores (NES) and Nominal (NOM) p value were calculated. NES is the primary statistic for examining GSEA results, it can be used to compare analysis results across gene sets. A positive NES indicates that the genes of the examined gene set is mostly represented at the top of the ranked list of genes, while negative NES indicates that the genes of the analysed gene set is mostly at the down of the ranked list of genes. The database is available at the Gene Expression Omnibus database at NCBI under the accession number GSE98114.

4. RESULTS

4.1 Cooperative effects of MASP-1 and other proinflammatory factors on endothelial inflammatory characteristics

4.1.1 Experimental setup

Various proinflammatory activators acting on endothelial cells (among others) can be present simultaneously or sequentially in the bloodstream during a bacterial (LPS and MASP-1) or viral (IFNγ and MASP-1) infection, in certain diseases such as hereditary angioedema (HAE) (bradykinin and MASP-1), or during an allergic reaction accompanied by a bacterial or fungal infection (histamine and MASP-1). Three possible interaction types were examined to investigate the potential cooperation with the complement lectin pathway and other coactivators. Cells were either cotreated with recombinant MASP-1 (rMASP-1) and one of the coactivators or pretreated with rMASP-1 and then treated with one of the coactivators or treated with rMASP-1 after pretreatment with one of the coactivators (**Figure 7**).
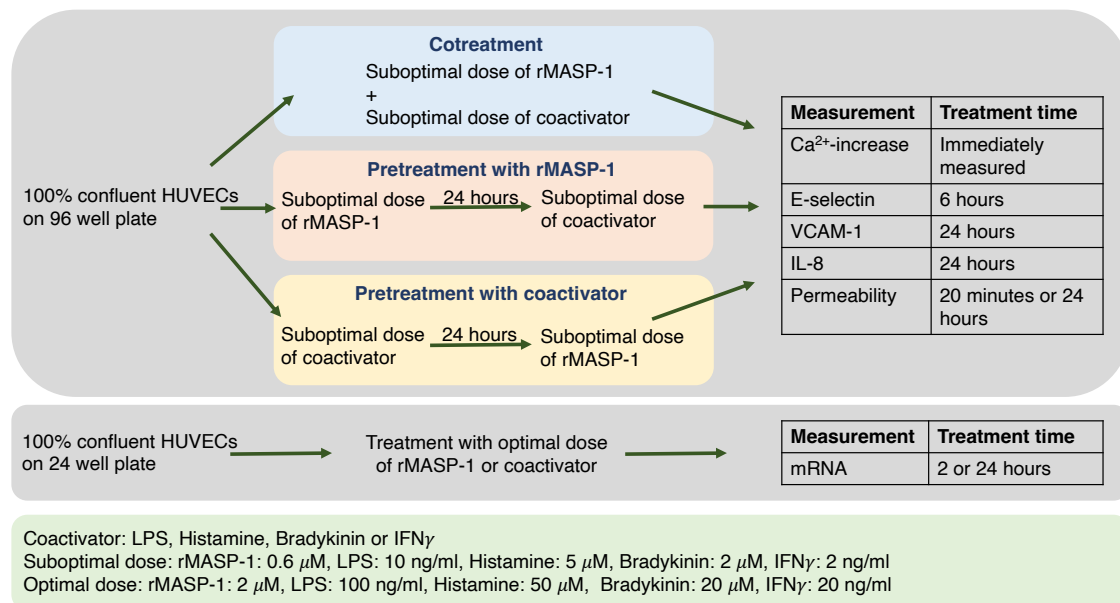

Figure 7. *A schematic overview of the experimental setup. The blue, pink, and yellow colors of the boxes representing the experimental setups are used for all subsequent figures for better understanding. Source of this figure is the candidate's own publication (20).*

These experimental setups model distinct pathophysiological conditions. The pretreatments always lasted for 24 hours, while treatment time varied depending on the measured parameter. Pre-established (17) suboptimal doses of treatments were used to ensure the possibility of an accurate measurement of the cellular response even when combined treatments were applied. Suboptimal dose refers to the concentration of the selected activator where we could observe an approximately half-maximum response according to our previous experiments.

We assessed cellular responses that we had previously demonstrated to be affected by MASP-1 either at mRNA or protein level in endothelial cells. Intracellular Ca^{2+}-mobilization initiates broad signaling through various activated receptors, including G-protein coupled protease activated receptors (PARs). The released IL-8 acts as a neutrophil chemoattractant, and adhesion molecules such as E-selectin and VCAM-1 facilitate the rolling and transmigration of leukocytes on endothelial cells, whereas increased vascular permeability ensures an effective extravasation of soluble immunological and acute phase mediators.

Given the substantial volume of generated data, in the followings, only those results are presented in detail, where significant cooperation could be found between MASP-1 and the various treatments. Nonetheless, we summarized the data obtained from every experimental setup in **Table 3**.

Table 3. *Cooperation between rMASP-1 and other coactivators. Various combinations of pretreatments and cotreatments were applied on the HUVECs, and several indicators of the endothelial cell activation were measured. An interaction was considered significant if the measured outcome of the combined treatment was statistically greater or smaller than the effect of each activator alone in the same experimental setup. All significant interactions ($p < 0.05$) that we found were positive (indicated by green coloring), and their directions are indicated by arrows.*

	Pretreatment	Treatment	Interaction				
			Ca^{2+}-mobilization	E-selectin	VCAM-1	IL-8	Permeability
Cotreatment		rMASP-1 + LPS		↑		↑	↑
		rMASP-1 + Histamine				↑	
		rMASP-1 + IFNγ				↑	
		rMASP-1 + Bradykinin					
Pretreatment with rMASP-1	rMASP-1	LPS					
	rMASP-1	Histamine	↑				
	rMASP-1	IFNγ					
	rMASP-1	Bradykinin	↑				
Pretreatment with coactivator	LPS	rMASP-1	↑	↑			↑
	Histamine	rMASP-1					
	IFNγ	rMASP-1	↑				
	Bradykinin	rMASP-1					

4.1.2 Ca^{2+}-mobilization

Ca^{2+}-mobilization plays a crucial role in the signal transduction of various receptors, including G protein-coupled histamine and bradykinin receptors (GPCRs) and protease-activated receptors (PARs). Fluo-4-AM is a calcium indicator, which exhibits increase in fluorescence upon binding Ca^{2+}, therefore enabling us to detect Ca^{2+}-mobilization in the cytosol. While LPS or IFNγ alone did not induce Ca^{2+}-mobilization in HUVECs, pre-treatment with either of these factors significantly enhanced the Ca^{2+}-mobilization response to rMASP-1 treatment (**Figure 8A and B**). Interestingly, cotreatment with MASP-1 with either BK or HA did not result in an increased Ca^{2+}-mobilization (data not

shown); however, both BK and HA elicited greater Ca^{2+}-mobilization in the HUVECs after rMASP-1 pretreatment (**Figure 8C and D**).
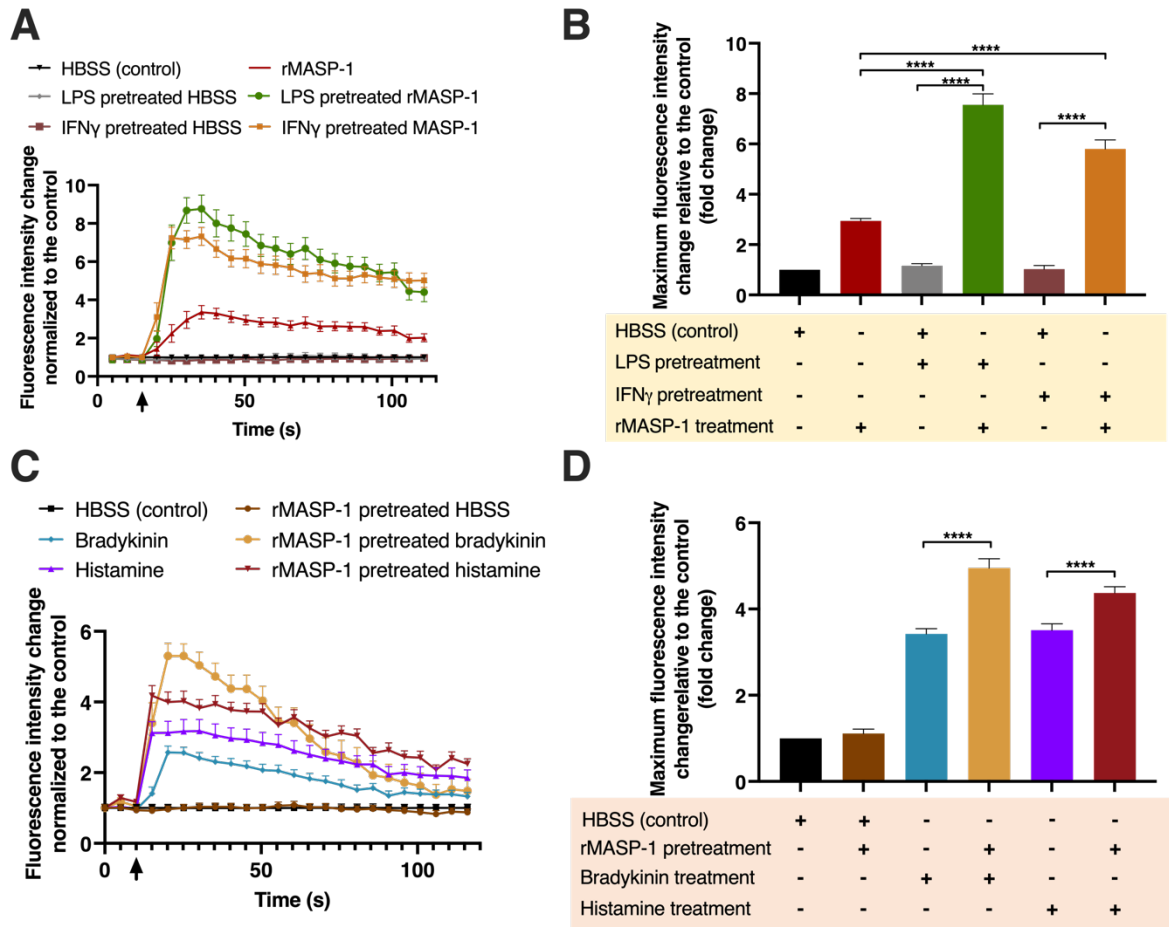

Figure 8. *MASP-1 interacted with LPS, IFNγ, histamine, and bradykinin to induce intracellular Ca^{2+}-mobilization in HUVECs. Confluent layers of HUVECs were cultured in 96-well plates and the cells were pretreated with LPS (10 ng/ml), IFNγ (2 ng/ml), bradykinin (2 μM), rMASP-1 (0.6 μM) or histamine (5 μM) for 24 hours or with medium alone (control). After the removal of pretreatment, the cells were loaded with 2 μM of Fluo-4-AM. Sequential images were taken by fluorescence microscopy every 5 seconds. Two images were taken initially to determine baseline fluorescence, then the treatment was applied, and the response was measured for 2 minutes. Left-side panels show data from a single, representative experiment, where fluorescence intensity values were background corrected and normalized to the control (**A, C**). Diagrams in the right-side panels show the means of maximum fluorescence intensity values from three independent experiments, normalized to the control. (**B**) LPS or IFNγ pretreatment was followed by rMASP-1 treatment. (**D**) rMASP-1 pretreatment was followed by bradykinin or histamine treatment. Compared to the control: HBSS vs. rMASP-1: **, HBSS vs. LPS pretreated*

HBSS: ns., HBSS vs. LPS pretreated rMASP-1: **, HBSS vs. IFNγ pretreated HBSS: ns., HBSS vs. IFNγ pretreated rMASP-1: **, HBSS vs. rMASP-1 pretreated HBSS: ns., HBSS vs. bradykinin: ****, HBSS vs. rMASP-1 pretreated bradykinin: ****, HBSS vs. histamine: ***, HBSS vs. rMASP-1 pretreated histamine: **** ; ↑: indicates the addition of the treatment; ns. non-significant; ** p < 0.01; *** p < 0.001; **** p < 0.0001. Source of this figure is the candidate's own publication (20).

4.1.3 Adhesion molecule expression

E-selectin and VCAM-1 are two important adhesion molecules; their expression indicate proinflammatory changes in the adhesion capacity of endothelial cells to leukocytes. LPS and rMASP-1 cooperated in the induction of E-selectin in two different ways, both the cotreatment and the LPS pretreatment followed by rMASP-1 treatment significantly increased the E-selectin levels in HUVECs (**Figures 9A, B**). No substantial cooperation in the induction of VCAM-1 was observed between rMASP-1 and the other activators.
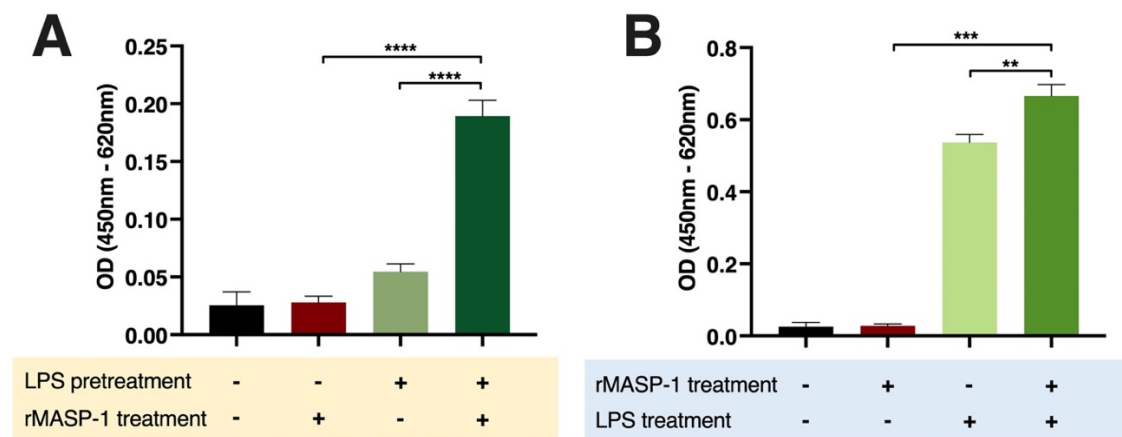

Figure 9. rMASP-1 cooperated with LPS in the induction of E-selectin on endothelial cells. Confluent layers of HUVECs were cultured in 96-well plates. (A): The cells were pretreated with LPS (10 ng/ml) for 24 hours, and after the removal of the pretreatment, rMASP-1 (0.6 µM) was added to the cells for 6 hours. (B): In the case of cotreatment, LPS (10 ng/ml) and rMASP-1 (0.6 µM) were added together to the cells for 6 hours. Then, the cells were fixed, and the expression level of E-selectin was determined by cell-based ELISA. Compared to the control: control vs. rMASP-1: ns., control vs. LPS pretreated control: ns., control vs. rMASP-1 treatment after LPS pretreatment: ****, control vs. LPS: ****, control vs. LPS + rMASP-1: ****; ns. non-significant; ** p < 0.01; *** p < 0.001; **** p < 0.0001. Source of this figure is the candidate's own publication (20).

4.1.4 IL-8 cytokine expression

Endothelial cells secrete IL-8, a chemokine, at a low constitutive rate, and its expression can be induced by various stimuli. The administration of LPS (24), histamine, or rMASP-1 (17) individually resulted in elevated IL-8 expression, while IFNγ did not induce such an effect on HUVECs. (**Figure 10**). Cotreating the cells with rMASP1 and LPS, or rMASP-1 and histamine significantly increased the yield of IL-8 secretion compared to the corresponding individual treatments. Interestingly, cotreatment with rMASP-1 and IFNγ also significantly increased IL-8 production of HUVECs (**Figure 10**).
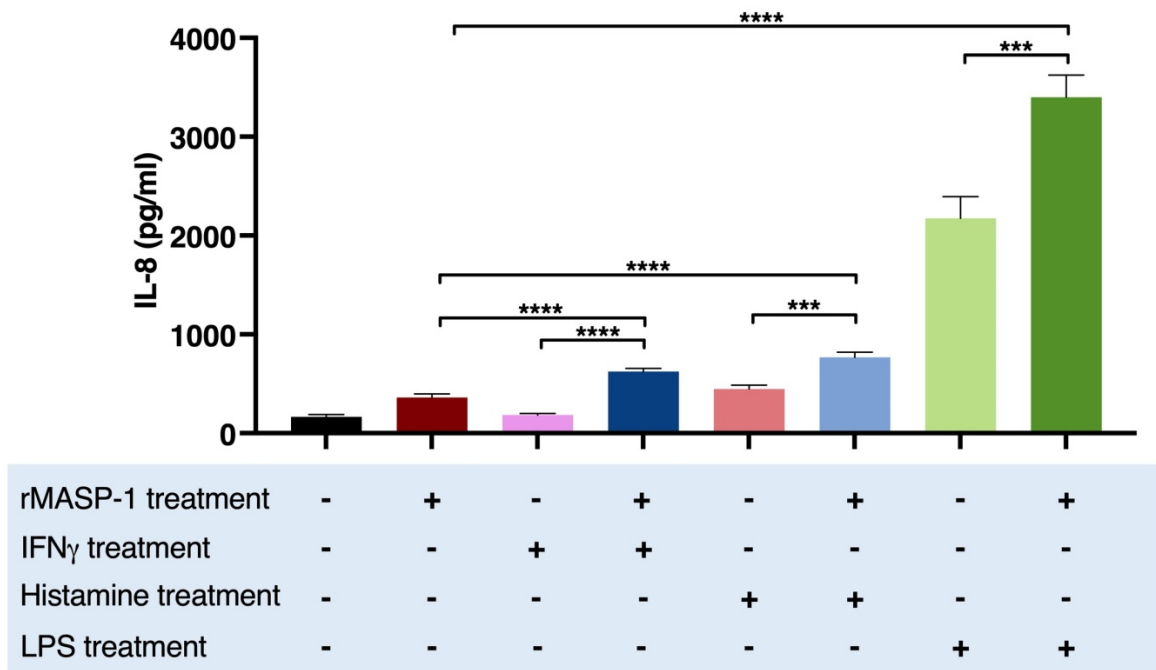

Figure 10. rMASP-1 interacted with IFNγ, histamine and LPS in the induction of IL-8 production of HUVECs. Confluent layers of HUVECs were cultured in 96-well plates and the cells were cotreated with rMASP-1 and LPS, histamine or IFNγ for 24 hours. The supernatants were collected and diluted in 1:20, then the IL-8 concentration was measured by sandwich ELISA. The results of the ELISAs were calculated from the standard curve and plotted as mean concentration values of three independent experiments. Compared to the control: control vs. rMASP-1: ****, control vs. IFNγ: ns., control vs. histamine: ****, control vs. LPS: ****; ns. non-significant; *** p < 0.001; **** p < 0.0001. Source of this figure is the candidate's own publication (20).

4.1.5 Permeability measurement

We used a modified version of XperT technique (19, 55) to measure the paracellular transport trough the endothelial layer. Using biotinylated gelatin and streptavidin-conjugated fluorescent dye, we could visualize and measure the size of the paracellular gaps. Both 24-hour-long LPS and rMASP-1 treatments alone increased permeability but the combination of the two treatments further opened the endothelial layer (**Figure 11**).
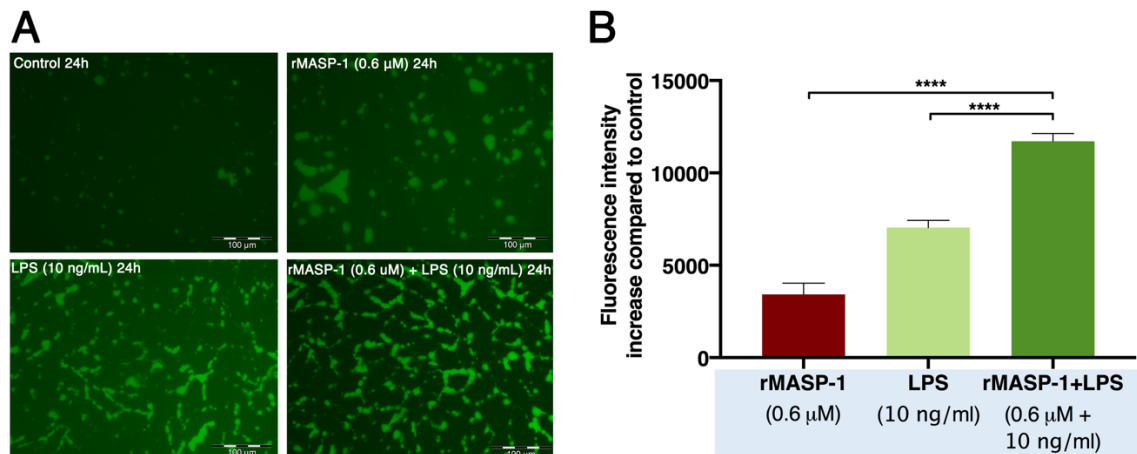

Figure 11. rMASP-1 and LPS cotreatment increased endothelial permeability. Confluent layers of HUVECs were cultured in 96-well plates pre-coated with biotinylated gelatin. The cells were treated with LPS (10 ng/ml), rMASP-1 (0.6 µM) or both, or with medium alone (control) for 24 hours. Cell-free areas of the surface of biotinylated gelatin were stained with Streptavidin-Alexa488, and after fixation, fluorescence was detected with a fluorescence plate-reader and representative images were taken using an Olympus IX-81 fluorescence microscope. A) Representative images of three independent experiments. The scale bar applies to all photos. B) Mean values of three independent experiments normalized to the controls, after background correction. Compared to the control: control vs. rMASP-1: ***; control vs. LPS: ****, control vs. rMASP-1 + LPS: ****; *** p < 0.001; **** p < 0.0001. Source of this figure is the candidate's own publication (20).

The rMASP-1 induced permeability in long- (24 hours) and short-term (20 minutes) and this dose-dependent increase could be further augmented by LPS pretreatment (**Figure 12**).
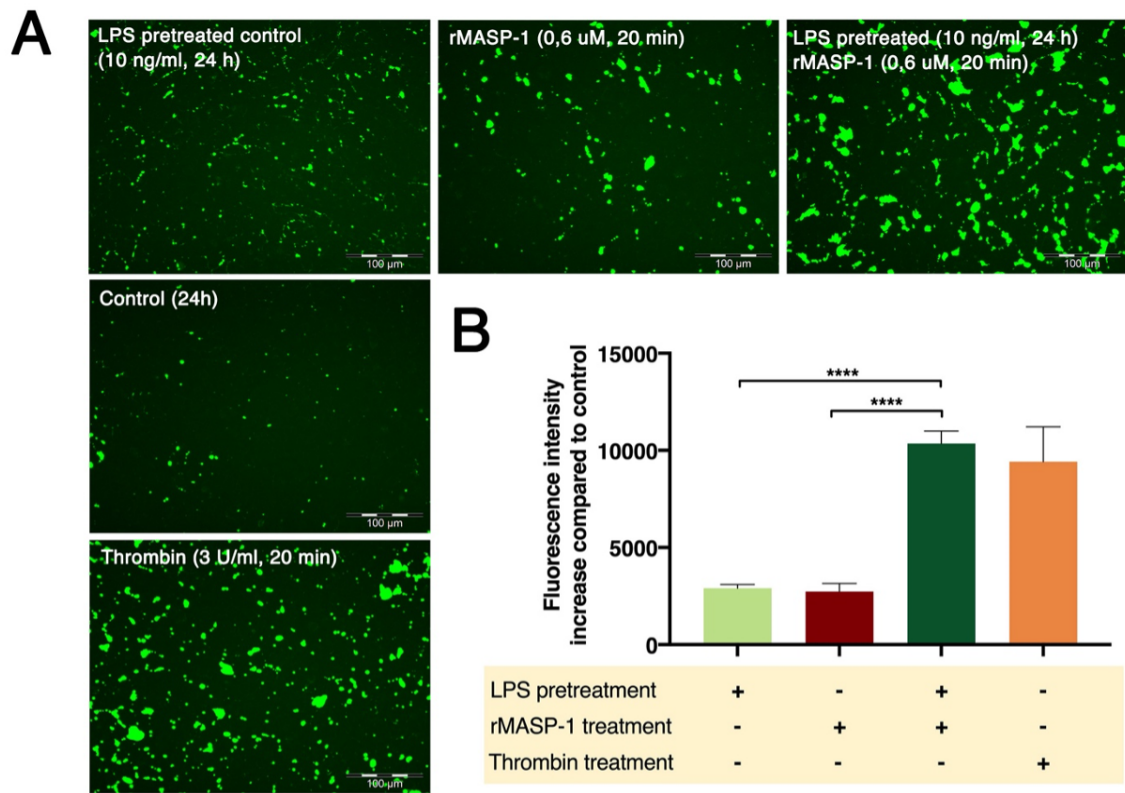

Figure 12. LPS pretreatment followed by rMASP-1 treatment increased endothelial permeability. Confluent layers of HUVECs were cultured in 96-well plates precoated with biotinylated gelatin. The cells were pretreated with LPS (10 ng/mL) or with medium alone (control) for 24 h, and then rMASP-1 treatment (0.6 µM) was added for 20 min. Thrombin (300 nM, 20 min) was used as a positive control. The cell-free areas of the biotinylated gelatin surface were stained with Streptavidin-Alexa488, and after fixation, fluorescence was detected with a fluorescence plate reader; representative images were taken using an Olympus IX-81 fluorescence microscope. (A) Representative images of three independent experiments. The scale bar applies to all photos. (B) Mean values of three independent experiments normalized to the controls after background correction. Compared to the control: control vs. LPS-pretreated control: ****, control vs. rMASP-1: ***, control vs. LPS-pretreated rMASP-1: ****, control vs. thrombin: ****; +: indicates that the pretreatment or treatment was added; -: indicates that pretreatment or treatment was not added; *** $p < 0.001$; **** $p < 0.0001$. Source of this figure is the candidate's own publication (20).

4.1.6 mRNA measurements for receptor expression

One of the simplest modes of collaboration is that pretreatment increases the expression of the receptor for the factor used subsequently. To evaluate this phenomenon, we measured the expression of histamine (HRH1), bradykinin (BDKRB1,2) and MASP-1 (PAR1,2 and 4) receptors, as their responsiveness was notably heightened by certain pretreatments.

As we demonstrated, rMASP-1 pretreatment potentiated the bradykinin-induced Ca^{2+}-mobilization in HUVECs (**Figure 8B**). Along with this, rMASP-1 significantly increased the mRNA levels of both B1 and B2 bradykinin receptors (BDKRB1 and 2) (**Figure 13A**).

Furthermore, rMASP-1 also increased the sensitivity of endothelial cells to histamine (**Figure 8B**), and although it was not statistically significant, we observed a tendency towards elevated mRNA levels in the H1 histamine receptor following a 2-hour long rMASP-1 treatment. (**Figure 13B**).

Pretreatment with LPS potentiated several cellular responses induced by rMASP-1 (Ca^{2+}-mobilization, E-selectin expression, and permeability); therefore, we measured the mRNA ex-pression of the three protease-activated receptors that could be activated by MASP-1. We found a strong increase in the PAR2 mRNA levels following a 24-hour LPS treatment (FC: 6.46), while the levels of the other two receptors remained unchanged (**Figure 13C**).

Besides LPS, IFNγ also enhanced rMASP-1-induced Ca^{2+}-mobilization. We observed interesting changes in the expression pattern of PAR receptors. The expression of PAR2 was downregulated after 2 hours (FC: 0.77, $p < 0.01$) and further decreased after 24 hours (FC: 0.49, $p < 0.001$), while PAR4 expression exhibited a slight decrease after 2 hours (FC: 0.59, $p < 0.05$), followed by a slight increase after 24 hours (FC: 1.58; although not statistically significant, the trend was apparent) (**Figure 13D**).
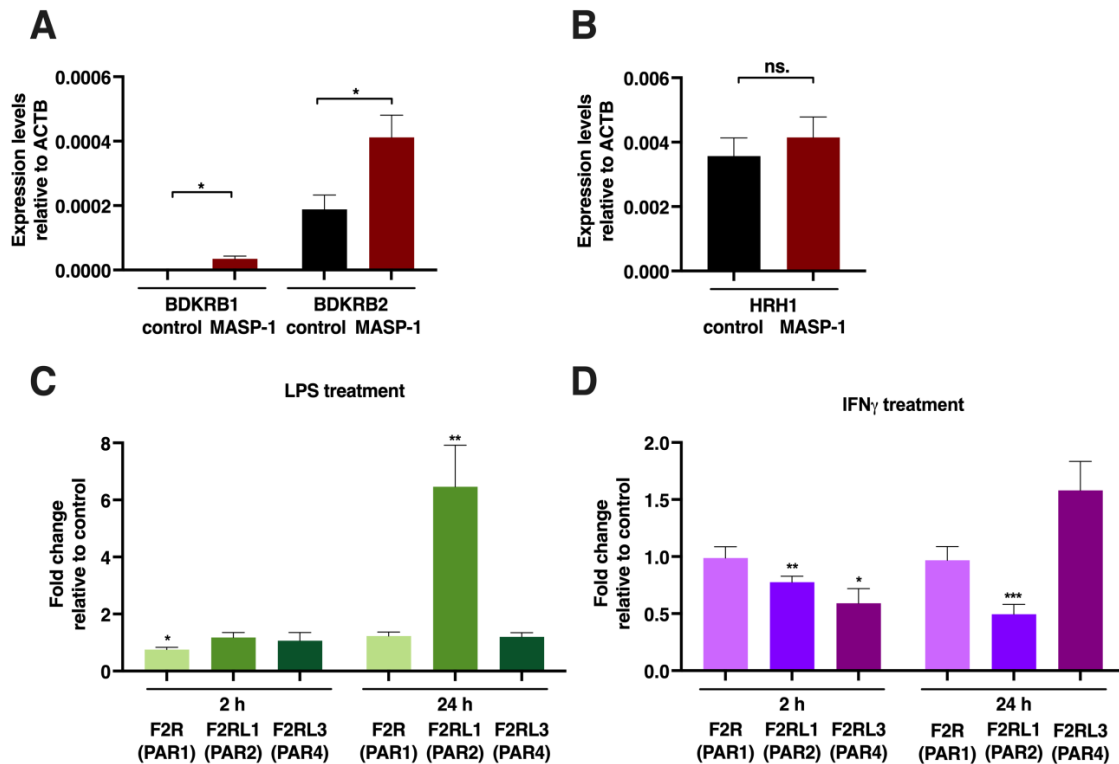
Figure 13. *rMASP-1, LPS and IFNγ changed the expression patterns of several endothelial cell receptors. Confluent layers of HUVECs were cultured in 24-well plates, and the cells were treated with rMASP-1 (2 μM), LPS (100 ng/mL), or IFNγ (20 ng/mL) for 2 or 24 h. RNA was purified, and after reverse transcription, quantitative PCR was performed using Qiagen Rotor-Gene Q. β-actin was used as an internal control.* ***A), B)*** *Relative expression levels of B1 and B2 bradykinin receptors (BDKRB1, 2) and the histamine H1 receptor (HRH1) after 2 h of rMASP-1 treatment. Data from three independent experiments.* ***C), D)*** *The effect of LPS or IFNγ treatment on the expressions of PARs 1, 2, and 4. The values represent the ratio of the expression level of treated vs. untreated control. One sample t-test was carried out to see if fold changes significantly differed from 1. Data from three independent experiments. * p < 0.05; ** p < 0.01; *** p < 0.001; ns: not significant. Source of this figure is the candidate's own publication (20).*

4.2 Cooperative effects of MASP-1 and mechanical wounding on endothelial wound healing processes

4.2.1 Experimental setup

In our experiments we studied the cellular effect of mechanical wounding on ECs as well as how the activation of MASP-1 modifies it and if the combination of the two activating signals induces a stronger response. When combined treatments (rMASP-1 + mechanical wounding) were applied, we used suboptimal dose (0.6 µM) of rMASP-1 to ensure the accurate measurement of the cellular response. When studying only the effect of rMASP-1, we used the normal dose (2 µM) as described in our previous research.

Our experimental setups model different pathophysiological conditions. When mechanical wounding is closely followed by rMASP-1 treatment it models the infection of a newly formed wound. When rMASP-1 treatment precedes mechanical wounding, it models a situation when the complement system is already activated by another stimuli.

4.2.2 Transcriptomic analysis

We have previously demonstrated that rMASP-1 significantly changes the expression of genes associated with inflammation and permeability (16, 19). Now, we investigated whether rMASP-1 alters the expression of wound healing- and angiogenesis-related genes using the same mRNA expression database (available in the NCBI Gene Expression Omnibus Database under accession number GSE98114). We utilized the Gene Ontology Annotation database to retrieve human genes from categories 'GO0001525 angiogenesis' (336 genes) and 'GO0042060 wound healing' (332 genes). Gene set enrichment analysis (GSEA) tests whether a given set of genes is represented as higher or lower in the ranked list of fold changes than the average fold changes of all genes. We found that both angiogenesis-related (normalized enrichment score (NES): 2.16, $p < 0.01$) and wound healing-related (NES:1.62, $p < 0.05$) genes were overrepresented at the top of the ranked list of genes after rMASP-1 treatment, which reflects significant upregulation of both wound-healing-related and angiogenesis-related gene sets in response to rMASP-1. We also found significant enrichment (NES:2.1, $p < 0.01$) when the genes of two categories were combined (603 genes).

Based on these findings, we further studied the wound healing and angiogenesis related processes of HUVEC cells, with particular attention to the involvement of rMASP-1.

4.2.3 Ca^{2+}-mobilization

As demonstrated earlier by others, mechanical wounding of endothelial cells induces a calcium wave that continues to propagate (56). We could also observe this by wounding the HUVEC layer with a sterile pipette tip. The response was rapid, initiated within seconds after scratching and propagated in a wave-like manner to neighboring cells. The intensity of Ca^{2+}-mobilization decreased with increasing distance from the initial wound. Apyrase (an ATP scavenger) did not inhibit the Ca^{2+}-mobilization closest to the wound but inhibited the propagation of the calcium wave from one cell to another (**Figure 14A**). As shown previously, rMASP-1 can also induce Ca^{2+}-mobilization in HUVECs (15) and this signaling process can be synergistically modified by other Ca^{2+}-mobilizing factors such as bradykinin, histamine (20) or hypoxia (21). We studied whether mechanical wounding induced Ca^{2+}-mobilization could also modify the Ca^{2+}-inducing potential of rMASP-1. In these experiments, we used suboptimal dose (0.6 μM) of rMASP-1 to ensure the accurate measurement of the cellular response. When administering rMASP-1 after mechanical injury, the rMASP-1 induced Ca^{2+}-mobilization was slightly inhibited, particularly in cells nearest to the wound and this inhibition remained consistent in the observed different time points (**Figure 14B**).
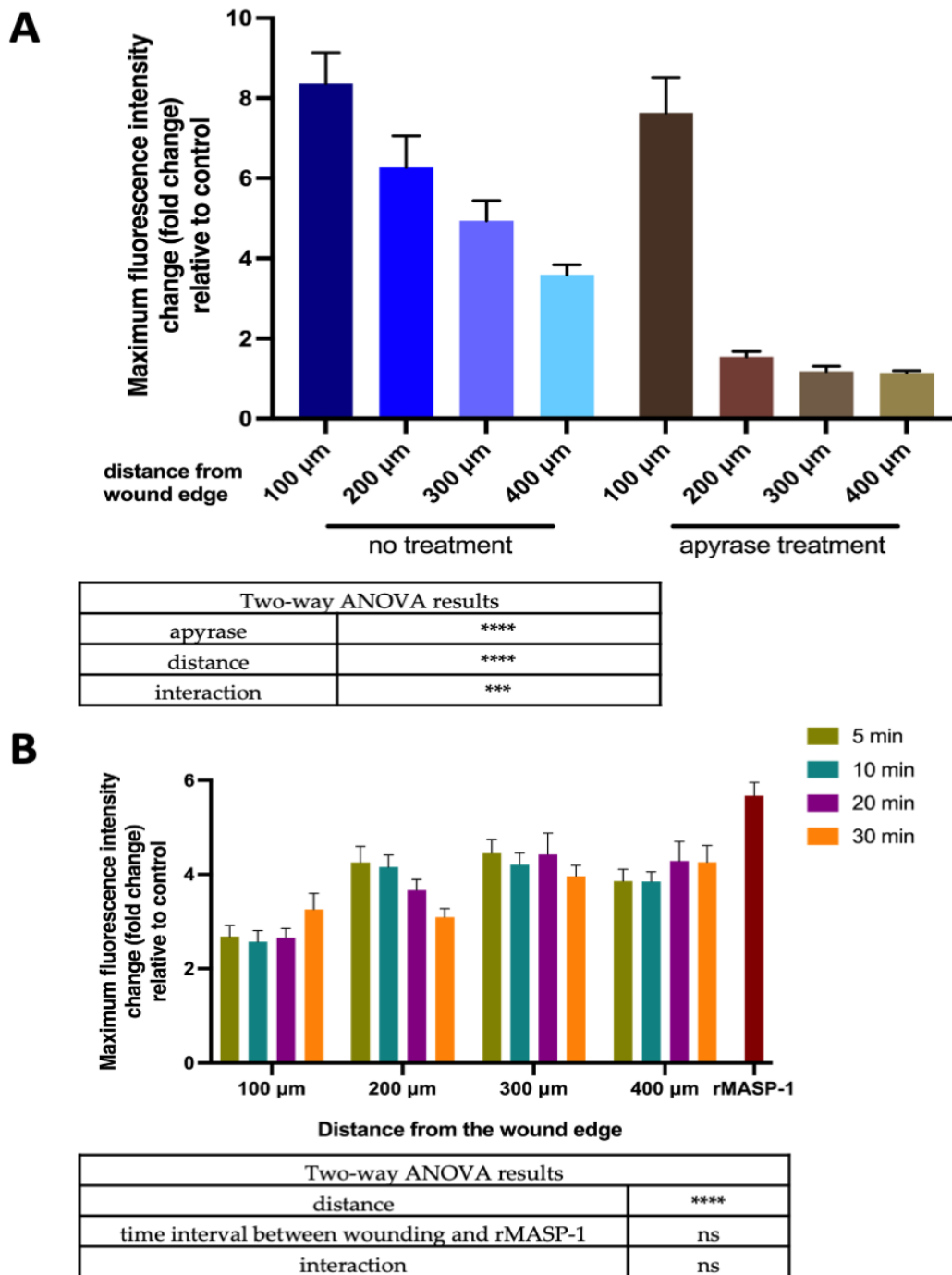
Figure 14. Ca^{2+}-mobilization in response to mechanical wounding and rMASP-1. *(a) Confluent layers of HUVECs were cultured in 96-well plates, and then cells were loaded with 2 μM of Fluo-4-AM. Sequential images were taken every 5 s using fluorescence microscopy. Initially, two images were taken to determine baseline fluorescence, and then HUVEC layers were scratched with a sterile pipette tip. The response was measured for 2 min. Apyrase treatment (10 U/mL) was applied 5 min before the measurement. (b) Cells were loaded with 2 μM of Fluo-4-AM and then scratched using a sterile pipette tip. Next, 0.6 μM of rMASP-1 treatment was added to the wells 5, 10, 20, or 30 min after scratching;*

then, sequential images were taken every 5 s using fluorescence microscopy. The effect of 0.6 μM of rMASP-1 without scratching was also measured for comparison. (a,b) Distances were measured from the edge of the initial wound. Before calculating the fold change values all images were background corrected and normalized to the control. Two-way ANOVA was used for statistical analysis. ****: p < 0.0001; ***: p < 0.001; ns: not significant. Source of this figure is the candidate's own publication (57).

4.2.4 CREB phosphorylation changes and NF-κB activation

To further study the effect of mechanical wounding on different signaling pathways we measured CREB phosphorylation and NF-κB activation (localization in the nucleus). CREB phosphorylation was measured 10, 15 or 30 minutes after wounding, and we observed the strongest after 15 minutes (**Figure 15A**). As we saw in the case of Ca^{2+}-mobilization, CREB phosphorylation was the most pronounced in the cells closest to the wound. Interestingly, apyrase pretreatment did not affect the wounding induced CREB phosphorylation. As we showed previously, rMASP-1 induces CREB phosphorylation (15). When mechanical wounding was closely followed (5 min) by rMASP-1 treatment, CREB phosphorylation was stronger than either the effect of rMASP-1 or wounding alone. The potentiating effect of rMASP-1 was independent of the distance of the wound edge (**Figure 15B**).

Two-way ANOVA results comparing different time points	
time	****
distance	****
interaction	****

Two-way ANOVA results to examine the effect of apyrase	
apyrase	ns
distance	****
interaction	ns

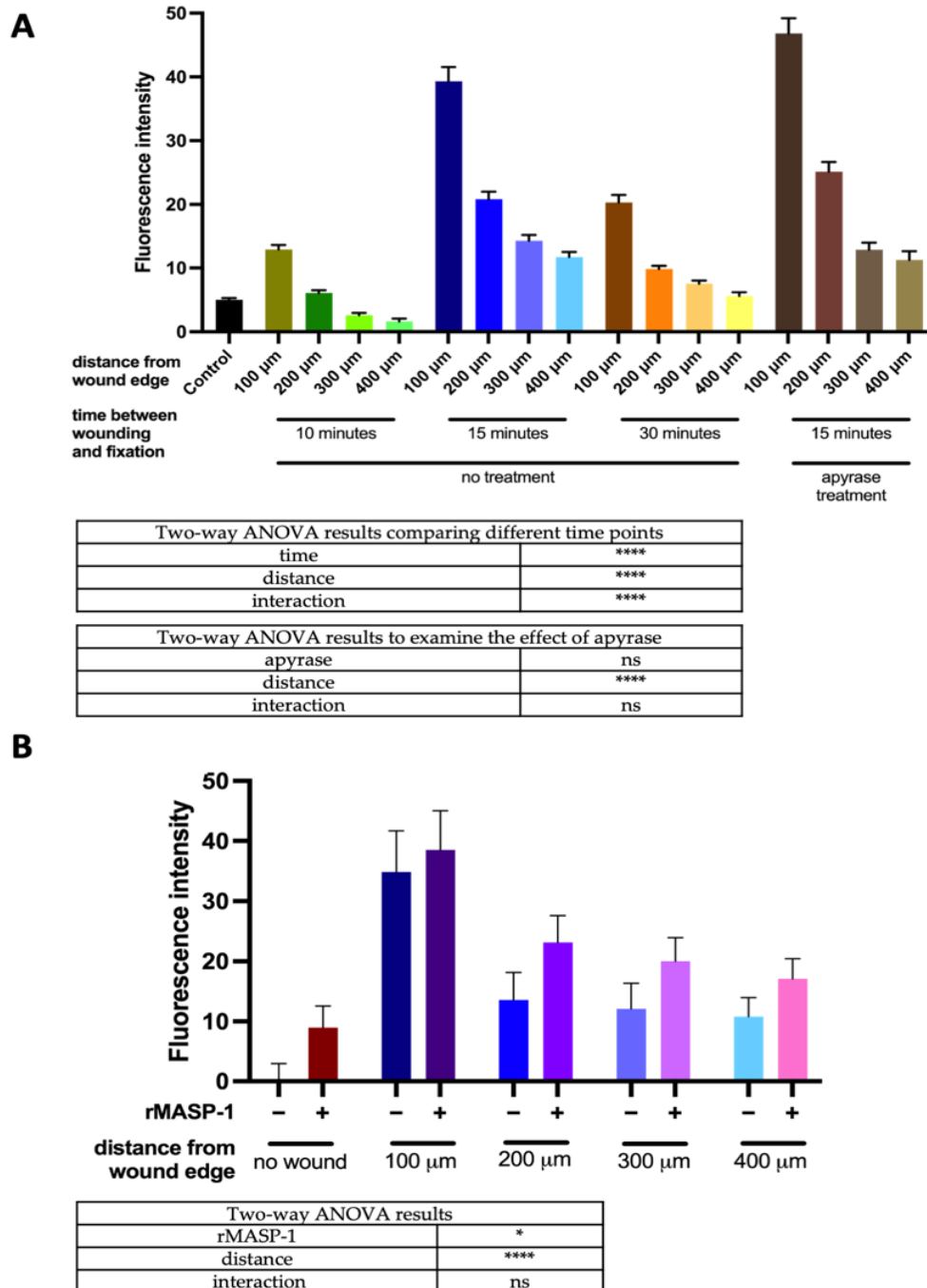| Two-way ANOVA results	
rMASP-1	*
distance	****
interaction	ns

Figure 15. Changes in CREB phosphorylation in response to wounding and rMASP-1. (a) Confluent layers of HUVECs were cultured in 96-well plates and scratched using a sterile pipette tip to create a wound. Apyrase treatment (10 U/mL) was applied 5 min before the wounding. Cells were fixed with ice-cold methanol–acetone (1:1) solution 10, 15, or 30 min after scratching. (b) The wells were scratched using a sterile pipette tip, and after 5 min, 0.6 µM of rMASP-1 was added to the wells. Cells were fixed with ice-cold methanol–acetone (1:1) 15 min after rMASP-1 treatment. (a,b) Cells were labeled with rabbit anti-human phospho-CREB antibody (1:200) and stained with goat anti-

rabbit Alexa568 (1:500) and Hoechst (1:50,000) nuclear staining. Images were taken using an Olympus IX-81 inverted fluorescence microscope, and the mean intensity of red fluorescence in the nuclear region was evaluated using CellP 5.2 software after background correction (Olympus Soft Imaging Solutions GmbH, 2011). Distances were measured from the edge of the initial wound. Two-way ANOVA was used for statistical analysis. ****: $p < 0.0001$; *: $p < 0.05$ ns: not significant. Source of this figure is the candidate's own publication (57).

The transcription factor NF-κB serves as a pivotal mediator of inflammatory responses therefore, its activation can be assumed during the inflammatory phase of the wound healing process. We studied the effect of mechanical wounding on NF-κB activation using NF-κB p65 antibody, but did not find any changes after 15, 30, 60 or 90 minutes (**Figure 16**).
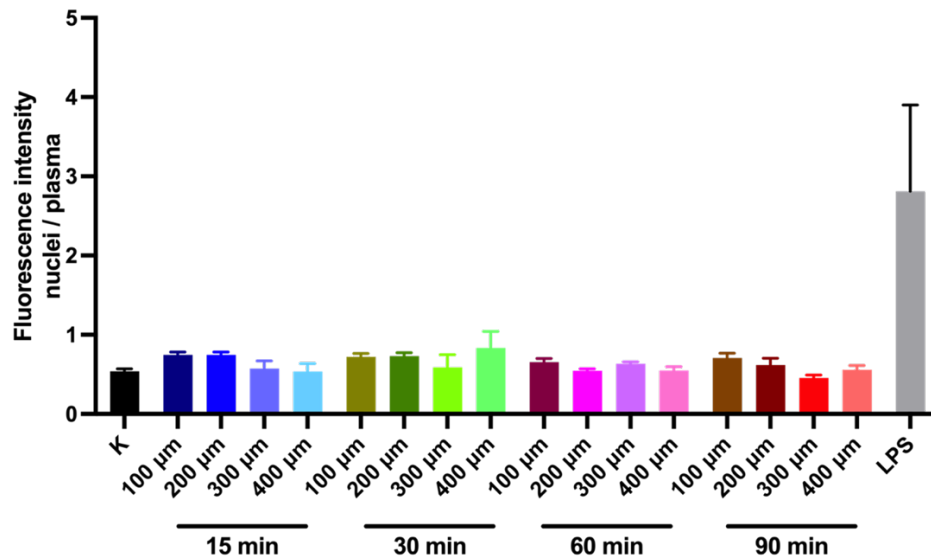

***Figure 16**. Effect of mechanical wounding on NF-κB activation. Confluent layers of HUVECs were cultured in 96-well plates and scratched using a sterile pipette tip to create a wound. Cells were fixed with ice-cold methanol-acetone (1:1) 15, 30, 60 or 90 minutes after scratching. We used 1 mg/ml LPS as a positive control. Cells were labelled with rabbit anti-human NF-κB p65 antibody (1:200) and stained with goat anti-rabbit Alexa568 (1:500) and Hoechst (1:50000) nuclear staining. Images were taken using an Olympus IX-81 inverted fluorescence microscope and the ratio of cytoplasmic and nuclear mean red fluorescence was evaluated using CellP software. Distances were measured from the edge of the initial wound. Source of this figure is the candidate's own publication (57).*

4.2.5 Expression of adhesion molecules

We utilized fluorescence microscopy to investigate the expression changes of three well-known adhesion molecules: E-selectin, ICAM-1 and VCAM-1, 6 and 24 hours after wounding. Mechanical wounding induced weak, but significant ICAM-1 and VCAM-1 expression at both time points (**Figure 17** and **18**). Although we could observe the induction of E-selectin expression 24 hours after wounding, it did not reach statistical significance (p=0.0504). Suboptimal dose of rMASP-1 induced ICAM-1 expression after 6 and 24 hours, VCAM-1 expression after 24 hours and E-selectin expression after 6 hours (**Figure 17** and **18**). When the two treatments were applied sequentially (24 hours long rMASP-1 pretreatment was followed by mechanical wounding) VCAM-1 expression was further induced (**Figure 18**).
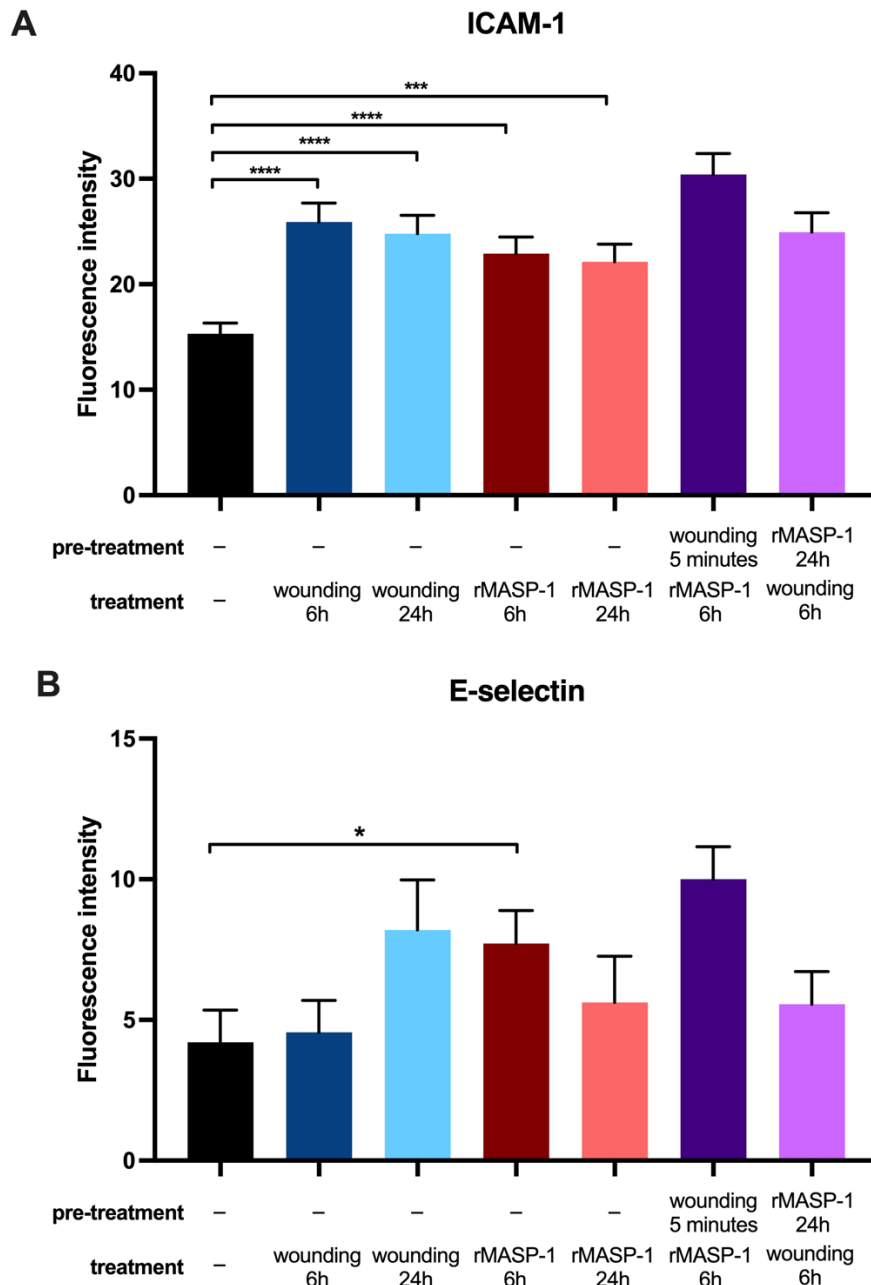
Figure 17. Changes in adhesion molecule expression in response to wounding and rMASP-1. Confluent layers of HUVECs were cultured in 96-well plates, and rMASP-1 pretreatment (0.6 μM) was applied to some of the wells. The wound was made using a sterile pipette tip. Cells were fixed after 6 or 24 h and then labeled with mouse anti-human ICAM-1 (a) or mouse anti-human E-selectin (b) antibodies (1:500) and stained with goat anti-mouse Alexa568 (1:500) and Hoechst (1:50,000) nuclear staining. Images were taken using an Olympus IX-81 inverted fluorescence microscope, and the mean intensity of red fluorescence in the cytoplasm was evaluated using CellP 5.2 software (Olympus Soft Imaging Solutions GmbH, 2011). ****: p < 0.0001; ***: p < 0.001; *: p < 0.05. Source of this figure is the candidate's own publication (57).
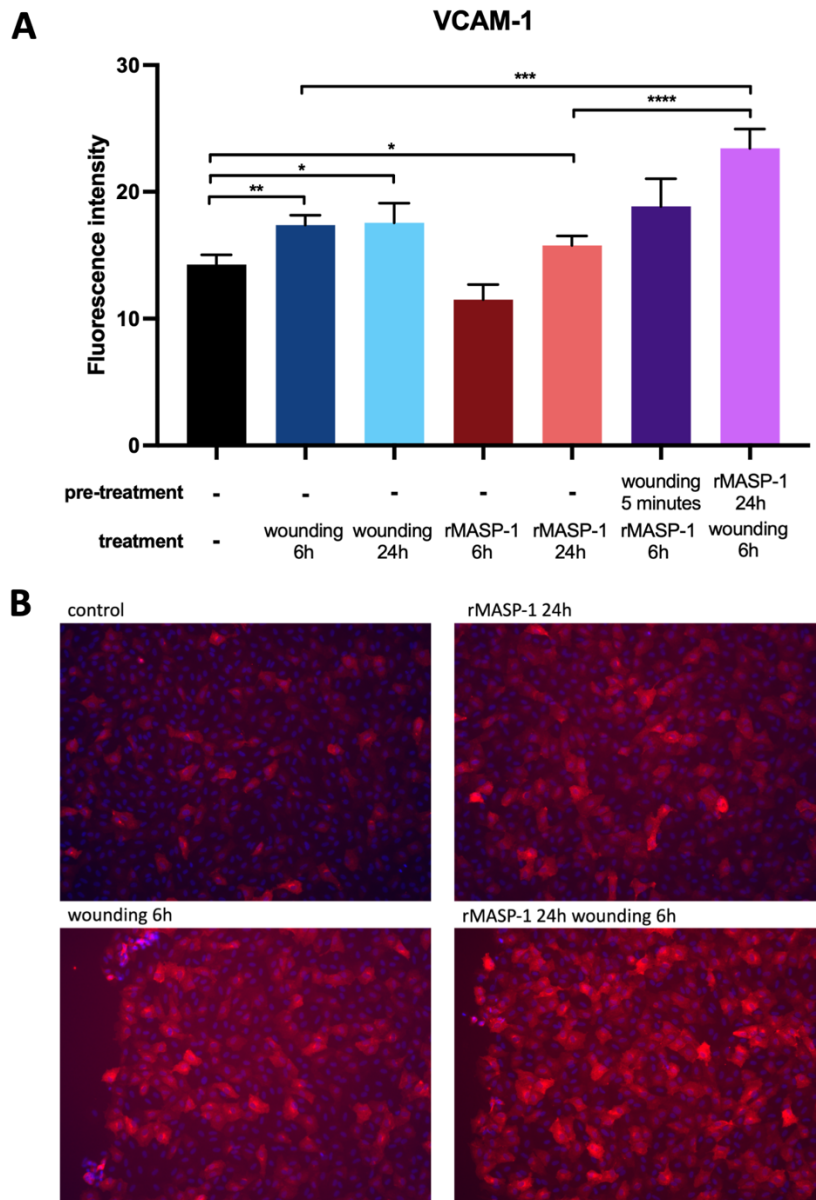
Figure 18. *Changes in VCAM-1 expression in response to wounding and rMASP-1. Confluent layers of HUVECs were cultured in 96-well plates, with rMASP-1 pretreatment (0.6 µM) applied to some of the wells. The wound was made using a sterile pipette tip. Cells were fixed after 6 or 24 h and then labeled with mouse anti-human VCAM-1 (1:500) and stained with goat anti-mouse Alexa568 (1:500) and Hoechst (1:50,000) nuclear staining. (a) Images were taken using an Olympus IX-81 inverted fluorescence microscope, and the mean intensity of red fluorescence in the cytoplasm was evaluated using CellP 3.4 software (Olympus Soft Imaging Solutions GmbH, 2011). Panel (b) shows representative images from three independent experiments. ****: $p < 0.0001$; ***: $p < 0.001$; **: $p < 0.01$; *: $p < 0.05$. Source of this figure is the candidate's own publication (57).*

4.2.6 Wound healing assay

We performed a wound repair assay to examine the pace of wound healing. We used 2 µM of rMASP-1 to study the individual effect (rather than the suboptimal dose used in previous experiments). We found that rMASP-1 did not affect the wound closure rate of HUVECs. Basic fibroblast growth factor (bFGF) was used as a positive control, which slightly but not significantly increased wound closure rate (**Figure 19**).
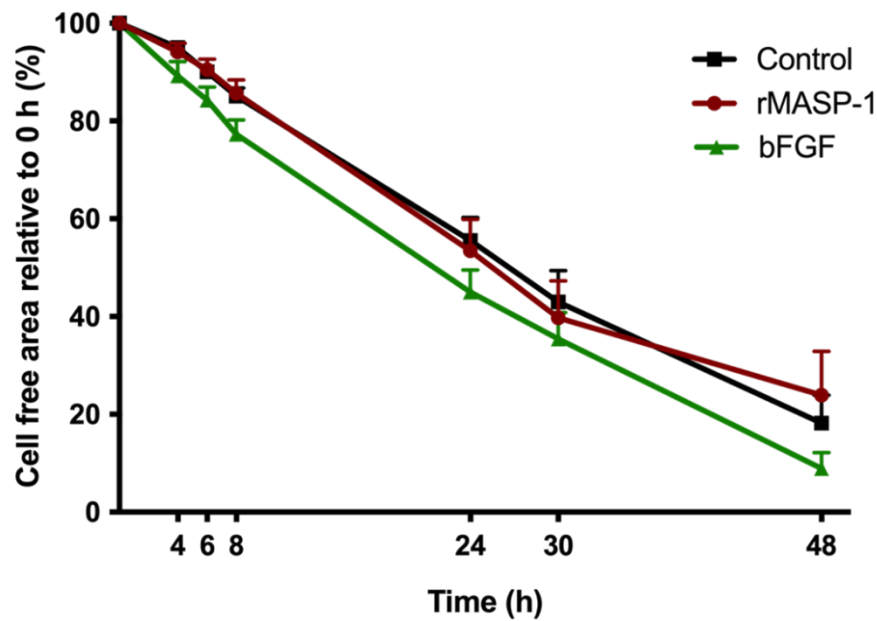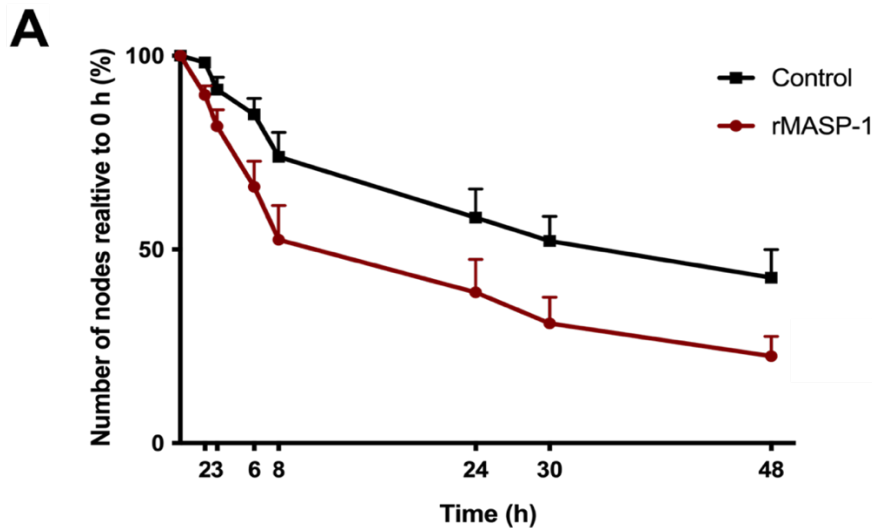

Two-way ANOVA results	
time	****
treatment	ns
interaction	ns

*Figure 19. Effect of rMASP-1 on wound closure rate. HUVEC cells were cultured in Ibidi 3-well culture inserts (which created a 500 µm wide cell-free area) until confluence, after which the inserts were removed, and the areas were photographed for 48 h. rMASP-1 (2 µM) or bFGF (1.6 ng/mL) was administered immediately after the removal of the inserts. We determined the size of the cell-free area using ImageJ software (1.54d) and plotted it against the 0 h time point. Two-way ANOVA was used for data analysis. ****: $p < 0.0001$; ns: not significant. Source of this figure is the candidate's own publication (57).*

4.2.7 Capillary networks on Matrigel

Matrigel® is a solubilized basement membrane matrix secreted by Engelbreth-Holm-Swarm mouse sarcoma cells which resembles the laminin/collagen IV-rich basement membrane found in many tissues. Cells cultured on Matrigel® exhibit complex cellular behavior that are otherwise challenging to observe in typical laboratory settings. Endothelial cells form a typical capillary-like network when they are seeded on Matrigel®. rMASP-1 treatment significantly accelerated the disintegration of this network compared to no-treatment control (**Figure 20**).
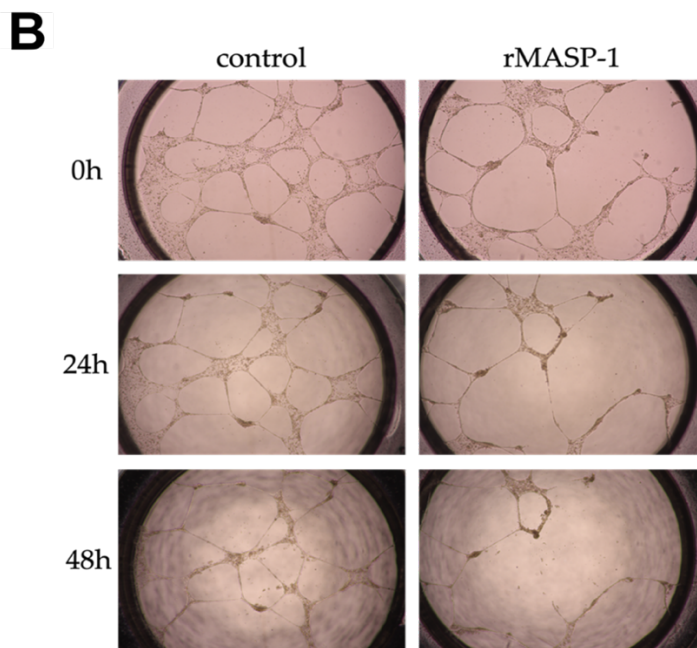
Figure 20. *Effect of rMASP-1 on capillary network integrity. HUVECs were seeded onto 15-well "Angiogenesis μ-Slides" coated with Matrigel® in 100% confluence and cultured for 16 h until typical capillary-like network structures were formed. The cells were then treated with 2 μM of rMASP-1. Photographs were taken 0, 2, 3, 5, 6, 8, 24, 30, and 48 h after treatment. (a) The number of nodes was determined using ImageJ software (1.54d) and then plotted against the number of nodes before treatment. Two-way ANOVA was utilized for data analysis. Panel (b) shows representative images from three independent experiments. ****: p < 0.0001; **: p < 0.01; ns: not significant. Source of this figure is the candidate's own publication (57).*

5. DISCUSSION

Endothelial cells participate in many physiological and pathological processes, and due to their location, they act as signal integrators. In *in vivo* situations, however, activating factors never act alone, therefore it is important to investigate the effect of MASP-1, the most abundant enzyme of complement lectin pathway, in combination with other proinflammatory stimuli.

As we are the first to examine the cooperation between MASP-1 and other proinflammatory activators, there is no specific literature available on this topic. Although information with the use of specific PAR inhibitors and thrombin is available, it is important to keep in mind that there are differences in the receptor usage of MASP-1 and thrombin. While MASP-1 cleaves PAR-1, -2 and -4 (15), thrombin cleaves PAR-1, -4 and possibly PAR-3, but not PAR-2 (58). The relative enzyme activity towards different PARs is also distinct in the case of MASP-1 and thrombin (15).

We found the most extensive cooperation between MASP-1 and LPS. Cotreating the HUVECs resulted in the induction of IL-8 and E-selectin expression, and increased permeability. In line with our findings, in airway epithelial cells, simultaneous LPS and PAR-1 agonist, PAR-2 agonist or thrombin treatment increased the expression of IL-8 more strongly than separate treatments did (59). The use of common signaling pathways may be behind this phenomenon (**Figure 21**). In our previous article, we demonstrated that predominantly the p38-MAPK pathway regulated the IL-8 production (17), and that LPS also induced p38-MAPK activation in HUVECs (24, 60). Besides the activation of p38-MAPK, Rallabandhi et al. showed that both PAR-2 agonist and LPS caused ERK 1/2 phosphorylation and increased the IL-8 and tissue factor (TF) expression at mRNA level in SW620 colonic epithelial cells (61). The NFAT signaling pathway also can be affected. Pan et al. found that LPS increased IL-8 production via the NFAT pathway in epithelial cells (62) and according to Jia et al., PAR-2 activation also promoted the nuclear translocation of NFAT (63). Regarding the regulation of permeability, we previously demonstrated that MASP-1 induced endothelial permeability via PAR-1 mediated intracellular Ca^{2+}-mobilization and Rho-kinase dependent myosin light chain (MLC) phosphorylation among others (19). Xie et al. showed that Rho-associated coiled-coil kinase (ROCK) inhibition decreased LPS induced permeability on HUVECs (64).
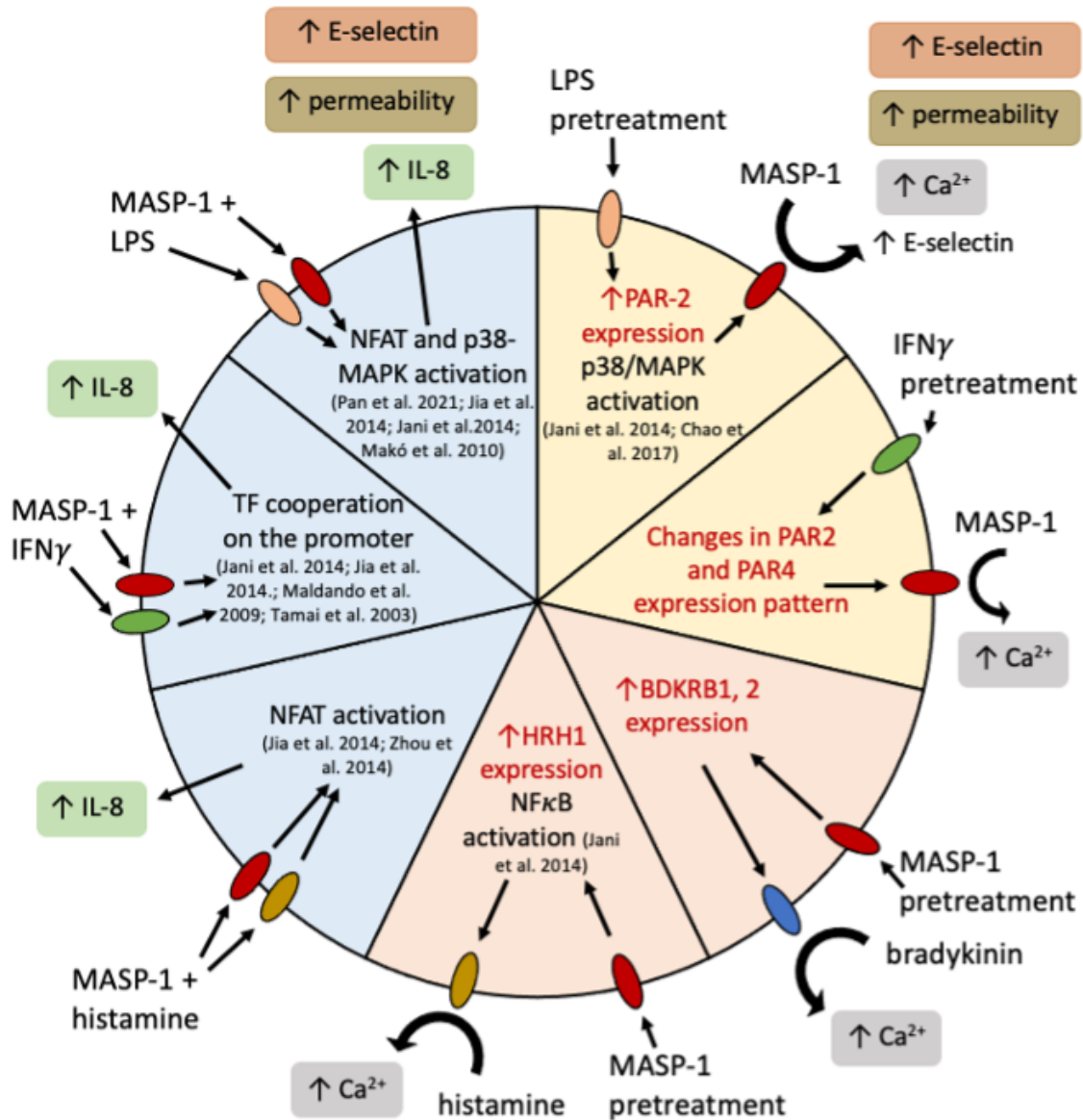
Figure 21. *MASP-1 and other proinflammatory activators cooperate in the induction of proinflammatory changes in endothelial cells. Yellow background indicates pretreatment with a coactivator followed by MASP-1 treatment, pink background indicates MASP-1 treatment followed by treatment with a coactivator, and blue background indicates cotreatment. Inside the circle, we indicated possible ways of cooperation. Red text signals results described in the present text; black text indicates data from literature. Blue oval: bradykinin receptor 2; red oval: PARs; green oval: IFNγ receptors 1 and 2; golden oval: histamine receptor 1; rose-colored oval: LBP/CD14/TLR4/MD2 receptor complex. Source of this figure is the candidate's own publication (20).*

Treating the endothelial cells with MASP-1 prior to the addition of LPS did not result in any significant changes in the measured responses. However, when we pretreated HUVECs with LPS and then added MASP-1, we observed significant cooperation in Ca^{2+}-mobilization, E-selectin expression, and the induction of permeability. Our mRNA level receptor expression measurements showed that LPS directly increased PAR-2 expression, which may explain the observed stronger reactions. In line with our findings, Chao et al. also found that LPS increased PAR-2 expression and Ca^{2+}-mobilization. MCP-1 expression and p38 phosphorylation were augmented in cells pretreated with LPS and subsequently treated with trypsin (which activates PAR-1, -2 and -4 (65)) (66). Besides receptor expression, the above-mentioned activation of common signaling pathways can also contribute to the observed cooperation.

MASP-1 elevated IL-8 production, whereas IFNγ treatment alone did not elicit IL-8 expression in HUVECs. Others also found that IL-8 production was not induced by IFNγ in HUVECs (67). Interestingly, the combined application of MASP-1 and IFNγ significantly increased IL-8 production compared to MASP-1 or IFNγ treatment alone. Consistent with our findings, Suk et al. demonstrated in the human monocytotic cell line U937, that IFNγ enhanced thrombin-triggered IL-8 production (68). In the absence of currently available data on the direct collaboration between IFNγ and PARs, we propose that the cooperation may manifest at the level of signaling pathways and/or the transcription factor usage within the IL-8 promoter region. The promoter region of IL-8 gene has binding sites for IFNγ-activated (e.g. IRFs, STAT1) and PAR-activated (e.g. NFAT, NFκB) transcription factors (69, 70).

Both MASP-1 and histamine alone increased IL-8 production in HUVECs, with their cotreatment further enhancing this response. Zhou et al. described that histamine induced IL-8 expression via the NFAT pathway in HUVECs (71). As previously mentioned, PAR-2 activation also promoted the nuclear translocation of NFAT, based on which we hypothesize that the stronger induction of the NFAT pathway may underline the observed increased IL-8 expression.

MASP-1 also affected the expression of bradykinin receptors; we found an increase in the mRNA levels of both bradykinin receptors (BDKRB1 and 2). In line with this, MASP-1 pretreatment enhanced Ca^{2+}-mobilization triggered by bradykinin treatment.

Following a 2-hour MASP-1 treatment we did not observe a significant increase in the histamine receptor (HRH1) expression, but there was a tendency towards it; and in line with this, we could observe increased Ca^{2+}-mobilization in response to histamine

treatment after MASP-1 pretreatment. As MASP-1 triggers the NF-κB pathway and the promoter region of HRH1 contains several NF-κB binding sites, it is possible that we would be able to find higher mRNA levels at later time points.

Pretreatment with IFNγ enhanced the Ca^{2+}-mobilization in response to MASP-1 treatment. Furthermore, we observed that IFNγ significantly altered the expression pattern of PAR-2 and PAR-4. Consistent with our results, Watanabe et al. demonstrated that pretreating HUVECs with IFNγ increased Ca^{2+}-mobilization (and prostacyclin production) when thrombin was used as secondary stimulator (72).

Inflammation is an integral part of the wound healing process, and the absence of the protective epidermis creates an opportunity for the entry of various microbes into the body. Therefore, wounding is a trivial pathophysiological state when different activation stimuli can modify the endothelial cells' response.

The identification of signals that initiate and direct endothelial wound healing responses is still a matter of active investigation. Immediately after wounding, endothelial cells initiate a Ca^{2+}-wave that originates at the wound edge and spreads towards the more distant areas of the monolayer. This phenomenon has been described in bovine corneal endothelial cells (BCENs) as well as in HUVECs (73, 74) (**Table 4**). In BCENs, apyrase treatment inhibited the propagation of Ca^{2+}-wave (73), whereas in HUVECs the scenario appears to be a somewhat more complicated. In contrast to our findings, apyrase did not inhibit laser-induced Ca^{2+}-wave propagation (75), which may be caused by the disparate induction method (laser vs. mechanical). Pohl et al. described that in the presence of apyrase only some of the neighboring cells took up the Ca^{2+}-wave, but alongside apyrase, gap junction blocker was also necessary to fully impede the mechanical stimulus-induced Ca^{2+}-wave (76). We confirmed that mechanical stimulation triggers a Ca^{2+}-wave in HUVECs and observed that cells nearest to the wound exhibited a Ca^{2+}-mobilization even in the presence of apyrase. However, the propagation of the Ca^{2+}-wave was inhibited. As we demonstrated earlier, MASP-1 initiates Ca^{2+}-mobilization in HUVECs. When MASP-1 treatment followed mechanical wounding, a secondary Ca^{2+}-mobilization was triggered. This response was smaller in magnitude compared to the effect of MASP-1 treatment alone, and the inhibition persisted for 30 minutes, particularly in the vicinity of the wound.

When activated by phosphorylation, cAMP response element binding protein (CREB) regulates the transcription of genes that regulate cellular metabolism, growth, migration, and proliferation in different cells and tissues (77). In Marine-Darby canine kidney cells

(MDCKs) and Swiss 3T3 fibroblasts, mechanical wounding induces CREB phosphorylation in the wounded and neighboring cells (78, 79). We demonstrated the first time that mechanical wounding triggers CREB phosphorylation in human endothelial cells. Earlier we had described that MASP-1 also induces CREB activation (15) and the current experiments showed that wounding and MASP-1 stimulus synergistically induce the phosphorylation of CREB. This suggests an enhanced activation response at the endothelial cell level when tissue damage is accompanied by microbial infection.

Table 4. Various cellular responses to mechanical wounding. We searched the literature for data available about the activation of signaling pathways and induced expression of adhesion molecules in response to mechanical wounding to compare with our results. * There was a clear tendency for increased E-selectin expression, but it did not reach statistical significance (p=0.00504).

Measured response	Literature data			Our data (HUVEC)
	Non-human	Human		
		non endothelial	endothelial	
Ca^{2+}-wave	yes (73) BCEN	yes (80) epithelial cells	yes (74) HUVEC	yes
CREB phosphorylation	yes (78, 79) MDCK, swiss 3t3 fibroblasts	no data	no data	yes
NF-κB activation	yes (81) rat and mouse endothelial cells	yes (82) keratinocytes	no (83) dermal endothelial cells	no
E-selectin	yes (84) rabbit skin	no data	yes (85) endothelial cells	no*
ICAM-1	yes (86) mouse skin	yes (87) keratinocytes	yes (87) endothelial cells	yes
VCAM-1	yes (81) rat and mouse endothelial cells	no data	yes (88) endothelial cells	yes

The NF-κB pathway activation is widely recognized as a participant in the regulation of inflammation that is part of the normal wound healing process. In rat and mouse aortas, Collins et al. observed NF-κB activation in endothelial cells at the leading edge 45 minutes after limited endothelial denudation (81). In human keratinocytes, mechanical wounding also induced NF-κB activation in the region of the leading edge 2 hours after wounding (82). In contrast, in human dermal endothelial cells, IκB, the inhibitory subunit of NF-κB, was activated following wounding (83). Consistent with this, we could not detect any NF-κB activation in HUVECs in response to mechanical damage.

The expression of various adhesion molecules on the surface of endothelial cells allows the transmigration of immune cells. Although it did not reach statistical significance, we could observe a tendency that mechanical wounding increased E-selectin expression. Consistently, Dreßler et al. found low to moderate staining on endothelial cells in injured human skin, while on uninjured skin E-selectin was not expressed (85). As we described, MASP-1 increased E-selectin expression 6 hours after treatment (18, 57), but we could not observe any cooperation between mechanical wounding and MASP-1.

Nagaoka et al. found that ICAM-1 is expressed by endothelial cells in the wounded skin of mice, and the loss of ICAM-1 inhibited the wound healing process (86). ICAM-1 is also expressed on the surface of endothelial cells in injured human skin (87). In line with these data, we demonstrated that mechanical wounding induces ICAM-1 expression on HUVECs, with its levels remaining elevated even a day after wounding.

Besides ICAM-1, VCAM-1 is also an important mediator of vascular adhesion and transendothelial migration of leukocytes (89). Collins et al. discovered localized VCAM-1 expression in rat and mouse aorta following limited endothelial denudation. This expression was confined to endothelial cells located immediately adjacent to the wound edge (81). In humans, Müller et al. observed that 18% of the endothelial cells in intact skin expressed VCAM-1 and only low intensity, whereas in injured skin, 51% of the endothelial cells were positive for VCAM-1 expression at higher intensities. They found the strongest expression of VCAM-1 occurring 4-6 hours after wounding (88). This aligns with our findings, we observed increased VCAM-1 levels in HUVEC 6 hours after wounding. In our previous transcriptomic studies, we detected elevated VCAM-1 mRNA expression (16), but surface VCAM-1 expression exhibited large individual variance (18, 21). When HUVECs were previously treated with MASP-1, wounding induced stronger VCAM-1 expression than the two treatments alone. It is possible that MASP-1 elevates

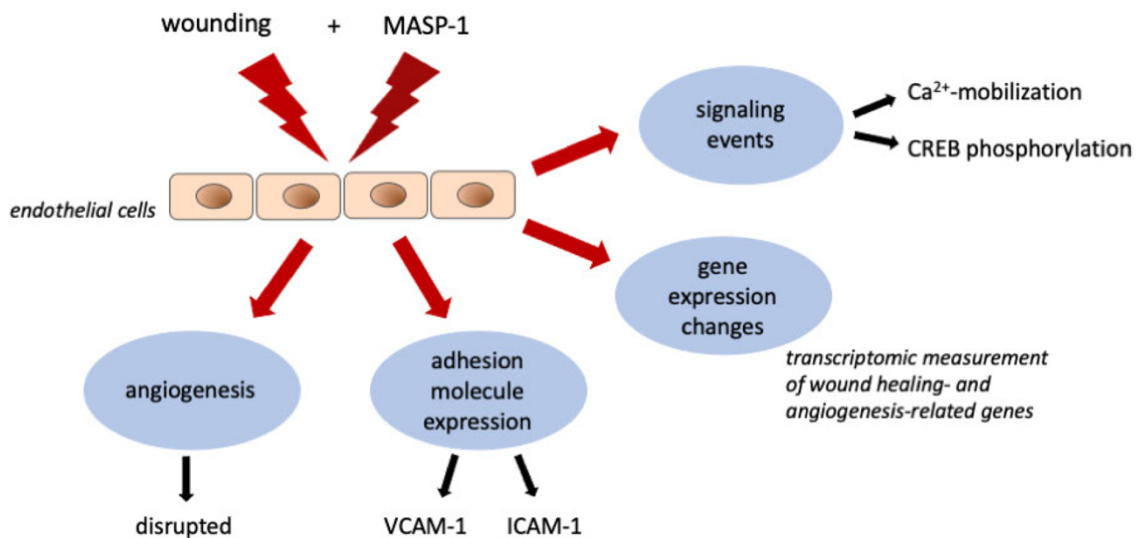VCAM-1 mRNA levels, and a subsequent stimulus, such as wounding, leads to elevated protein expression.

Figure 22. Complement MASP-1 modifies endothelial wound healing at several levels: signaling events, transcriptomic changes, adhesion molecule expression, and complex functional outcomes (e.g. angiogenesis). Source of this figure is the candidate's own publication (57).

A key indicator of the success of the wound healing process, is the time needed for wound closure. Svensson et al. described that neither PAR-1 nor PAR-2 agonists enhanced the rate of wound healing in HUVECs (90), and wound closure in PAR-1 deficient mice is normal (91). Consistently, we found that MASP-1 (using PAR-1, -2 and -4 signaling pathways in HUVEC) did not affect the rate of wound closure.

During the proliferation phase of wound healing, the integrity of the capillary network is restored with suitable angiogenesis. It has been reported that thrombin and PAR-1 activating peptide inhibited endothelial tube formation, while PAR-2 activator peptide had no effect on it (92, 93). In our research we found that MASP-1 accelerated the disintegration of the endothelial network (**Figure 22**).

DOI:10.14753/SE.2025.3135

6. CONCLUSIONS

During my doctoral studies, I studied the cooperative effects of MASP-1 and other activating signals on endothelial cell behavior. As endothelial cells play a substantial role in the regulation of inflammation by balancing pro- and anti-inflammatory states, minor effects on endothelial cell activation can cause major inflammatory changes. Despite the use of suboptimal doses of all activators, we found several situations where Ca^{2+}-mobilization, the permeability of the endothelial layer, and the expression of cytokines and adhesion molecules were significantly enhanced by the treatments. These collaborative interactions may reduce the threshold of endothelial cells to danger signals by augmenting receptor expressions and the stronger activation of signaling pathways. Particularly, we found considerable types of cooperation between MASP-1 and LPS, highlighting the risks of bacterial infections under conditions where the complement system was already activated or easily triggered.

Wounding is one of the most trivial inductors of inflammation, as microbes can easily enter the body through the wound. Our experiments provide a simplified model of mechanical wounding accompanied with complement MASP-1 activation (which can be triggered by various pathogens and altered host cells). Besides, our findings broaden the general knowledge of endothelial wound healing in terms of the participating signaling pathways and the expression induction of adhesion molecules.

We found that MASP-1 can modify the endothelial cells immediate response to wounding (second Ca^{2+}-mobilization, stronger CREB phosphorylation, gene expression changes), their participation in the inflammatory phase (increased VCAM-1 expression) and the later occurring proliferation phase (disruption of angiogenesis).

Our results suggest that the activation of MASP-1 has a different outcome in the different stages of wound healing. Inflammation is part of the normal wound healing process, but its resolution is essential, as persisting inflammation leads to the development of a chronic, non-healing wounds. MASP-1 promotes a proinflammatory phenotype which can be beneficial in the early stages, but harmful later.

These interactions described in our articles highlight the importance of studying the combined effects of different activating factors and considering endothelial cells as signal integrators, who participate greatly in the defense mechanisms of our bodies.

7. SUMMARY

Endothelial cells (ECs) constitute the innermost layer of the vessel walls. They act as signal integrators, creating the adequate respond to the various molecules present in the blood and play a crucial role in wound healing processes after injury. MASP-1, the most abundant enzyme of complement lectin pathway induces a proinflammatory phenotype in ECs and its activation is triggered by different pathogens or altered host cells. An inflammatory response is also an integral part of the wound healing process, and the participation of the complement lectin pathway is an actively researched topic.

Our aim was to investigate the combined effect of MASP-1 and different activating factors (LPS, histamine, bradykinin and IFNγ) in the induction of proinflammatory phenotype in ECs. We also studied the cellular effect of mechanical wounding in the presence or absence of MASP-1, as an evident model for proinflammatory activation.

We demonstrated that MASP-1 cooperated with all the above-mentioned activating factors in a variety of ways. LPS pretreatment increased the expression of PAR-2, a MASP-1 receptor, and furthermore, MASP-1 and LPS enhanced each other's effects in regulating IL-8, E-selectin, Ca^{2+}-mobilization, and changes in permeability. We showed that cotreatment of MASP-1 and IFNγ increased the IL-8 expression of ECs. Moreover, MASP-1 induced bradykinin and histamine receptor expression, and consequently, increased Ca^{2+}-mobilization was found. Pretreatment with IFNγ enhanced MASP-1-induced Ca^{2+}-mobilization. Mechanical wounding induced a Ca^{2+}-wave, CREB phosphorylation and the expression of adhesion molecules on ECs. We found that MASP-1 can modify the ECs immediate response to wounding (second Ca^{2+}-answer, stronger CREB phosphorylation, gene expression changes), their participation in the inflammatory phase (increased VCAM-1 expression) and the later occurring proliferation phase (disruption of angiogenesis).

Our findings highlight that well-known proinflammatory mediators and MASP-1 can strongly synergize to enhance the inflammatory response of ECs. Particularly, we found considerable types of cooperation between MASP-1 and LPS, highlighting the risks of bacterial infections under conditions where the complement system was already activated or easily triggered. MASP-1 can also modify the ECs participation in wound healing processes. Our data suggest that MASP-1 promoting a proinflammatory phenotype can be beneficial in the early stages, but harmful later as persisting inflammation can lead to the development of chronic wounds.

8. REFERENCES

1.   Cines DB, Pollak ES, Buck CA, Loscalzo J, Zimmerman GA, McEver RP, et al. Endothelial cells in physiology and in the pathophysiology of vascular disorders. Blood. 1998;91(10):3527-61.

2.   Aird WC. Phenotypic heterogeneity of the endothelium: I. Structure, function, and mechanisms. Circ Res. 2007;100(2):158-73.

3.   Sandoo A, van Zanten JJ, Metsios GS, Carroll D, Kitas GD. The endothelium and its role in regulating vascular tone. Open Cardiovasc Med J. 2010;4:302-12.

4.   Munoz-Chapuli R, Quesada AR, Angel Medina M. Angiogenesis and signal transduction in endothelial cells. Cell Mol Life Sci. 2004;61(17):2224-43.

5.   Shao Y, Saredy J, Yang WY, Sun Y, Lu Y, Saaoud F, et al. Vascular Endothelial Cells and Innate Immunity. Arterioscler Thromb Vasc Biol. 2020;40(6):e138-e52.

6.   Dobo J, Pal G, Cervenak L, Gal P. The emerging roles of mannose-binding lectin-associated serine proteases (MASPs) in the lectin pathway of complement and beyond. Immunol Rev. 2016;274(1):98-111.

7.   Dobo J, Schroeder V, Jenny L, Cervenak L, Zavodszky P, Gal P. Multiple roles of complement MASP-1 at the interface of innate immune response and coagulation. Mol Immunol. 2014;61(2):69-78.

8.   Teillet F, Gaboriaud C, Lacroix M, Martin L, Arlaud GJ, Thielens NM. Crystal structure of the CUB1-EGF-CUB2 domain of human MASP-1/3 and identification of its interaction sites with mannan-binding lectin and ficolins. J Biol Chem. 2008;283(37):25715-24.

9.   Dobo J, Harmat V, Beinrohr L, Sebestyen E, Zavodszky P, Gal P. MASP-1, a promiscuous complement protease: structure of its catalytic region reveals the basis of its broad specificity. J Immunol. 2009;183(2):1207-14.

10.   Krarup A, Gulla KC, Gal P, Hajela K, Sim RB. The action of MBL-associated serine protease 1 (MASP1) on factor XIII and fibrinogen. Biochim Biophys Acta. 2008;1784(9):1294-300.

11.   Hess K, Ajjan R, Phoenix F, Dobo J, Gal P, Schroeder V. Effects of MASP-1 of the complement system on activation of coagulation factors and plasma clot formation. PLoS One. 2012;7(4):e35690.

12.   Jenny L, Dobo J, Gal P, Schroeder V. MASP-1 of the complement system promotes clotting via prothrombin activation. Mol Immunol. 2015;65(2):398-405.

13.   Jenny L, Dobo J, Gal P, Schroeder V. MASP-1 Induced Clotting--The First Model of Prothrombin Activation by MASP-1. PLoS One. 2015;10(12):e0144633.

14.   Dobo J, Major B, Kekesi KA, Szabo I, Megyeri M, Hajela K, et al. Cleavage of kininogen and subsequent bradykinin release by the complement component: mannose-binding lectin-associated serine protease (MASP)-1. PLoS One. 2011;6(5):e20036.

15.   Megyeri M, Mako V, Beinrohr L, Doleschall Z, Prohaszka Z, Cervenak L, et al. Complement protease MASP-1 activates human endothelial cells: PAR4 activation is a link between complement and endothelial function. J Immunol. 2009;183(5):3409-16.

16.   Schwaner E, Nemeth Z, Jani PK, Kajdacsi E, Debreczeni ML, Doleschall Z, et al. Transcriptome analysis of inflammation-related gene expression in endothelial cells activated by complement MASP-1. Sci Rep. 2017;7(1):10462.

17.   Jani PK, Kajdacsi E, Megyeri M, Dobo J, Doleschall Z, Futosi K, et al. MASP-1 induces a unique cytokine pattern in endothelial cells: a novel link between complement system and neutrophil granulocytes. PLoS One. 2014;9(1):e87104.

18.   Jani PK, Schwaner E, Kajdacsi E, Debreczeni ML, Ungai-Salanki R, Dobo J, et al. Complement MASP-1 enhances adhesion between endothelial cells and neutrophils by up-regulating E-selectin expression. Mol Immunol. 2016;75:38-47.

19.   Debreczeni ML, Nemeth Z, Kajdacsi E, Schwaner E, Mako V, Masszi A, et al. MASP-1 Increases Endothelial Permeability. Front Immunol. 2019;10:991.

20.   Nemeth Z, Debreczeni ML, Kajdacsi E, Dobo J, Gal P, Cervenak L. Cooperation of Complement MASP-1 with Other Proinflammatory Factors to Enhance the Activation of Endothelial Cells. Int J Mol Sci. 2023;24(11).

21.   Demeter F, Nemeth Z, Kajdacsi E, Bihari G, Dobo J, Gal P, et al. Detrimental interactions of hypoxia and complement MASP-1 in endothelial cells as a model for atherosclerosis-related diseases. Sci Rep. 2024;14(1):14882.

22.   Fujihara M, Muroi M, Tanamoto K, Suzuki T, Azuma H, Ikeda H. Molecular mechanisms of macrophage activation and deactivation by lipopolysaccharide: roles of the receptor complex. Pharmacol Ther. 2003;100(2):171-94.

23.   Dauphinee SM, Karsan A. Lipopolysaccharide signaling in endothelial cells. Lab Invest. 2006;86(1):9-22.

24.   Mako V, Czucz J, Weiszhar Z, Herczenik E, Matko J, Prohaszka Z, et al. Proinflammatory activation pattern of human umbilical vein endothelial cells induced by IL-1beta, TNF-alpha, and LPS. Cytometry A. 2010;77(10):962-70.

25. Bannerman DD, Goldblum SE. Mechanisms of bacterial lipopolysaccharide-induced endothelial apoptosis. Am J Physiol Lung Cell Mol Physiol. 2003;284(6):L899-914.

26. Fox RH, Goldsmith R, Kidd DJ, Lewis GP. Bradykinin as a vasodilator in man. J Physiol. 1961;157(3):589-602.

27. Farmer PJ, Bernier SG, Lepage A, Guillemette G, Regoli D, Sirois P. Permeability of endothelial monolayers to albumin is increased by bradykinin and inhibited by prostaglandins. Am J Physiol Lung Cell Mol Physiol. 2001;280(4):L732-8.

28. Dobrivojevic M, Spiranec K, Sindic A. Involvement of bradykinin in brain edema development after ischemic stroke. Pflugers Arch. 2015;467(2):201-12.

29. Bae SW, Kim HS, Cha YN, Park YS, Jo SA, Jo I. Rapid increase in endothelial nitric oxide production by bradykinin is mediated by protein kinase A signaling pathway. Biochem Biophys Res Commun. 2003;306(4):981-7.

30. Li H, Burkhardt C, Heinrich UR, Brausch I, Xia N, Forstermann U. Histamine upregulates gene expression of endothelial nitric oxide synthase in human vascular endothelial cells. Circulation. 2003;107(18):2348-54.

31. Parsons ME, Ganellin CR. Histamine and its receptors. Br J Pharmacol. 2006;147 Suppl 1(Suppl 1):S127-35.

32. Ng CT, Fong LY, Abdullah MNH. Interferon-gamma (IFN-gamma): Reviewing its mechanisms and signaling pathways on the regulation of endothelial barrier function. Cytokine. 2023;166:156208.

33. Ellis S, Lin EJ, Tartar D. Immunology of Wound Healing. Curr Dermatol Rep. 2018;7(4):350-8.

34. Aird WC. Spatial and temporal dynamics of the endothelium. J Thromb Haemost. 2005;3(7):1392-406.

35. van Hinsbergh VW. Endothelium--role in regulation of coagulation and inflammation. Semin Immunopathol. 2012;34(1):93-106.

36. Petri B, Sanz MJ. Neutrophil chemotaxis. Cell Tissue Res. 2018;371(3):425-36.

37. Velnar T, Gradisnik L. Tissue Augmentation in Wound Healing: the Role of Endothelial and Epithelial Cells. Med Arch. 2018;72(6):444-8.

38. Herman IM. Molecular mechanisms regulating the vascular endothelial cell motile response to injury. J Cardiovasc Pharmacol. 1993;22 Suppl 4:S25-36.

39. van Hinsbergh VW, Collen A, Koolwijk P. Role of fibrin matrix in angiogenesis. Ann N Y Acad Sci. 2001;936:426-37.

40.   O'Kane S. Wound remodelling and scarring. J Wound Care. 2002;11(8):296-9.

41.   Liu T, Zhang L, Joo D, Sun SC. NF-kappaB signaling in inflammation. Signal Transduct Target Ther. 2017;2:17023-.

42.   Wen AY, Sakamoto KM, Miller LS. The role of the transcription factor CREB in immune function. J Immunol. 2010;185(11):6413-9.

43.   Mayr B, Montminy M. Transcriptional regulation by the phosphorylation-dependent factor CREB. Nat Rev Mol Cell Biol. 2001;2(8):599-609.

44.   Shaywitz AJ, Greenberg ME. CREB: a stimulus-induced transcription factor activated by a diverse array of extracellular signals. Annu Rev Biochem. 1999;68:821-61.

45.   Ollivier V, Parry GC, Cobb RR, de Prost D, Mackman N. Elevated cyclic AMP inhibits NF-kappaB-mediated transcription in human monocytic cells and endothelial cells. J Biol Chem. 1996;271(34):20828-35.

46.   Parry GC, Mackman N. Role of cyclic AMP response element-binding protein in cyclic AMP inhibition of NF-kappaB-mediated transcription. J Immunol. 1997;159(11):5450-6.

47.   Fumagalli S, Perego C, Zangari R, De Blasio D, Oggioni M, De Nigris F, et al. Lectin Pathway of Complement Activation Is Associated with Vulnerability of Atherosclerotic Plaques. Front Immunol. 2017;8:288.

48.   Pavlov VI, Tan YS, McClure EE, La Bonte LR, Zou C, Gorsuch WB, et al. Human mannose-binding lectin inhibitor prevents myocardial injury and arterial thrombogenesis in a novel animal model. Am J Pathol. 2015;185(2):347-55.

49.   Cazander G, Jukema GN, Nibbering PH. Complement activation and inhibition in wound healing. Clin Dev Immunol. 2012;2012:534291.

50.   Megyeri M, Harmat V, Major B, Vegh A, Balczer J, Heja D, et al. Quantitative characterization of the activation steps of mannan-binding lectin (MBL)-associated serine proteases (MASPs) points to the central role of MASP-1 in the initiation of the complement lectin pathway. J Biol Chem. 2013;288(13):8922-34.

51.   Megyeri M, Jani PK, Kajdacsi E, Dobo J, Schwaner E, Major B, et al. Serum MASP-1 in complex with MBL activates endothelial cells. Mol Immunol. 2014;59(1):39-45.

52.   Oroszlan M, Herczenik E, Rugonfalvi-Kiss S, Roos A, Nauta AJ, Daha MR, et al. Proinflammatory changes in human umbilical cord vein endothelial cells can be induced neither by native nor by modified CRP. Int Immunol. 2006;18(6):871-8.

53.	Schneider CA, Rasband WS, Eliceiri KW. NIH Image to ImageJ: 25 years of image analysis. Nat Methods. 2012;9(7):671-5.

54.	Subramanian A, Tamayo P, Mootha VK, Mukherjee S, Ebert BL, Gillette MA, et al. Gene set enrichment analysis: a knowledge-based approach for interpreting genome-wide expression profiles. Proc Natl Acad Sci U S A. 2005;102(43):15545-50.

55.	Dubrovskyi O, Birukova AA, Birukov KG. Measurement of local permeability at subcellular level in cell models of agonist- and ventilator-induced lung injury. Lab Invest. 2013;93(2):254-63.

56.	Demer LL, Wortham CM, Dirksen ER, Sanderson MJ. Mechanical stimulation induces intercellular calcium signaling in bovine aortic endothelial cells. Am J Physiol. 1993;264(6 Pt 2):H2094-102.

57.	Nemeth Z, Demeter F, Dobo J, Gal P, Cervenak L. Complement MASP-1 Modifies Endothelial Wound Healing. Int J Mol Sci. 2024;25(7).

58.	Altrogge LM, Monard D. An assay for high-sensitivity detection of thrombin activity and determination of proteases activating or inactivating protease-activated receptors. Anal Biochem. 2000;277(1):33-45.

59.	Ostrowska E, Reiser G. Protease-activated receptor (PAR)-induced interleukin-8 production in airway epithelial cells requires activation of MAP kinases p44/42 and JNK. Biochem Biophys Res Commun. 2008;366(4):1030-5.

60.	Hippenstiel S, Soeth S, Kellas B, Fuhrmann O, Seybold J, Krull M, et al. Rho proteins and the p38-MAPK pathway are important mediators for LPS-induced interleukin-8 expression in human endothelial cells. Blood. 2000;95(10):3044-51.

61.	Rallabhandi P, Nhu QM, Toshchakov VY, Piao W, Medvedev AE, Hollenberg MD, et al. Analysis of proteinase-activated receptor 2 and TLR4 signal transduction: a novel paradigm for receptor cooperativity. J Biol Chem. 2008;283(36):24314-25.

62.	Pan HY, Ladd AV, Biswal MR, Valapala M. Role of Nuclear Factor of Activated T Cells (NFAT) Pathway in Regulating Autophagy and Inflammation in Retinal Pigment Epithelial Cells. Int J Mol Sci. 2021;22(16).

63.	Jia X, Zhang H, Cao X, Yin Y, Zhang B. Activation of TRPV1 mediates thymic stromal lymphopoietin release via the Ca2+/NFAT pathway in airway epithelial cells. FEBS Lett. 2014;588(17):3047-54.

64.	Xie K, Wang W, Chen H, Han H, Liu D, Wang G, et al. Hydrogen-Rich Medium Attenuated Lipopolysaccharide-Induced Monocyte-Endothelial Cell Adhesion and

Vascular Endothelial Permeability via Rho-Associated Coiled-Coil Protein Kinase. Shock. 2015;44(1):58-64.

65.   Heuberger DM, Schuepbach RA. Protease-activated receptors (PARs): mechanisms of action and potential therapeutic modulators in PAR-driven inflammatory diseases. Thromb J. 2019;17:4.

66.   Chao HH, Chen PY, Hao WR, Chiang WP, Cheng TH, Loh SH, et al. Lipopolysaccharide pretreatment increases protease-activated receptor-2 expression and monocyte chemoattractant protein-1 secretion in vascular endothelial cells. J Biomed Sci. 2017;24(1):85.

67.   Beck GC, Yard BA, Breedijk AJ, Van Ackern K, Van Der Woude FJ. Release of CXC-chemokines by human lung microvascular endothelial cells (LMVEC) compared with macrovascular umbilical vein endothelial cells. Clin Exp Immunol. 1999;118(2):298-303.

68.   Suk K, Cha S. Thrombin-induced interleukin-8 production and its regulation by interferon-gamma and prostaglandin E2 in human monocytic U937 cells. Immunol Lett. 1999;67(3):223-7.

69.   Tamai R, Sugawara S, Takeuchi O, Akira S, Takada H. Synergistic effects of lipopolysaccharide and interferon-gamma in inducing interleukin-8 production in human monocytic THP-1 cells is accompanied by up-regulation of CD14, Toll-like receptor 4, MD-2 and MyD88 expression. J Endotoxin Res. 2003;9(3):145-53.

70.   Maldonado-Perez D, Brown P, Morgan K, Millar RP, Thompson EA, Jabbour HN. Prokineticin 1 modulates IL-8 expression via the calcineurin/NFAT signaling pathway. Biochim Biophys Acta. 2009;1793(7):1315-24.

71.   Zhou MH, Zheng H, Si H, Jin Y, Peng JM, He L, et al. Stromal interaction molecule 1 (STIM1) and Orai1 mediate histamine-evoked calcium entry and nuclear factor of activated T-cells (NFAT) signaling in human umbilical vein endothelial cells. J Biol Chem. 2014;289(42):29446-56.

72.   Watanabe K, Tanaka H, Wen FQ, Yoshida M. Effect of cytokines on thrombin-stimulated increases in intracellular calcium and PGI2 production by cultured human umbilical vein endothelial cells. Cell Signal. 1996;8(4):247-51.

73.   D'Hondt C, Ponsaerts R, Srinivas SP, Vereecke J, Himpens B. Reduced intercellular communication and altered morphology of bovine corneal endothelial cells with prolonged time in cell culture. Curr Eye Res. 2009;34(6):454-65.

74. Junkin M, Lu Y, Long J, Deymier PA, Hoying JB, Wong PK. Mechanically induced intercellular calcium communication in confined endothelial structures. Biomaterials. 2013;34(8):2049-56.

75. Atkinson BT, Jasuja R, Chen VM, Nandivada P, Furie B, Furie BC. Laser-induced endothelial cell activation supports fibrin formation. Blood. 2010;116(22):4675-83.

76. Kameritsch P, Pogoda K, Ritter A, Munzing S, Pohl U. Gap junctional communication controls the overall endothelial calcium response to vasoactive agonists. Cardiovasc Res. 2012;93(3):508-15.

77. Guan CX, Cui YR, Sun GY, Yu F, Tang CY, Li YC, et al. Role of CREB in vasoactive intestinal peptide-mediated wound healing in human bronchial epithelial cells. Regul Pept. 2009;153(1-3):64-9.

78. Togo T. Cell membrane disruption stimulates NO/PKG signaling and potentiates cell membrane repair in neighboring cells. PLoS One. 2012;7(8):e42885.

79. Togo T. Long-term potentiation of wound-induced exocytosis and plasma membrane repair is dependent on cAMP-response element-mediated transcription via a protein kinase C- and p38 MAPK-dependent pathway. J Biol Chem. 2004;279(43):44996-5003.

80. Klepeis VE, Cornell-Bell A, Trinkaus-Randall V. Growth factors but not gap junctions play a role in injury-induced Ca2+ waves in epithelial cells. J Cell Sci. 2001;114(Pt 23):4185-95.

81. Lindner V, Collins T. Expression of NF-kappa B and I kappa B-alpha by aortic endothelium in an arterial injury model. Am J Pathol. 1996;148(2):427-38.

82. Na J, Lee K, Na W, Shin JY, Lee MJ, Yune TY, et al. Histone H3K27 Demethylase JMJD3 in Cooperation with NF-kappaB Regulates Keratinocyte Wound Healing. J Invest Dermatol. 2016;136(4):847-58.

83. Chaudhuri V, Potts BR, Karasek MA. Mechanisms of microvascular wound repair I. Role of mitosis, oxygen tension, and I-kappa B. In Vitro Cell Dev Biol Anim. 2006;42(10):308-13.

84. Nwariaku FE, Mileski WJ, Lightfoot E, Jr., Sikes PJ, Lipsky PE. Alterations in leukocyte adhesion molecule expression after burn injury. J Trauma. 1995;39(2):285-8.

85. Dressler J, Bachmann L, Koch R, Muller E. Enhanced expression of selectins in human skin wounds. Int J Legal Med. 1998;112(1):39-44.

86. Nagaoka T, Kaburagi Y, Hamaguchi Y, Hasegawa M, Takehara K, Steeber DA, et al. Delayed wound healing in the absence of intercellular adhesion molecule-1 or L-selectin expression. Am J Pathol. 2000;157(1):237-47.

87. Dressler J, Bachmann L, Kasper M, Hauck JG, Muller E. Time dependence of the expression of ICAM-1 (CD 54) in human skin wounds. Int J Legal Med. 1997;110(6):299-304.

88. Dressler J, Bachmann L, Koch R, Muller E. Estimation of wound age and VCAM-1 in human skin. Int J Legal Med. 1999;112(3):159-62.

89. O'Brien KD, Allen MD, McDonald TO, Chait A, Harlan JM, Fishbein D, et al. Vascular cell adhesion molecule-1 is expressed in human coronary atherosclerotic plaques. Implications for the mode of progression of advanced coronary atherosclerosis. J Clin Invest. 1993;92(2):945-51.

90. Svensson KJ, Kucharzewska P, Christianson HC, Skold S, Lofstedt T, Johansson MC, et al. Hypoxia triggers a proangiogenic pathway involving cancer cell microvesicles and PAR-2-mediated heparin-binding EGF signaling in endothelial cells. Proc Natl Acad Sci U S A. 2011;108(32):13147-52.

91. Connolly AJ, Suh DY, Hunt TK, Coughlin SR. Mice lacking the thrombin receptor, PAR1, have normal skin wound healing. Am J Pathol. 1997;151(5):1199-204.

92. Chan B, Merchan JR, Kale S, Sukhatme VP. Antiangiogenic property of human thrombin. Microvasc Res. 2003;66(1):1-14.

93. Fortunato TM, Vara DS, Wheeler-Jones CP, Pula G. Expression of protease-activated receptor 1 and 2 and anti-tubulogenic activity of protease-activated receptor 1 in human endothelial colony-forming cells. PLoS One. 2014;9(10):e109375.

9. BIBLIOGRAPHY OF THE CANDIDATE'S PUBLICATIONS

9.1 Publications on which the dissertation is based

1. Z Németh, ML Debreczeni, E Kajdácsi, J Dobó, P Gál, L Cervenak

    Cooperation of complement MASP-1 with other proinflammatory factors to enhance the activation of endothelial cells

    Int. J. Mol. Sci., 2023, 24(11):9181, doi: 10.3390/ijms24119181, PMID: 37298134

    IF: 4.9

2. Z Németh, F Demeter, J Dobó, P Gál, L Cervenak

    Complement MASP-1 modifies endothelial wound healing

    Int. J. Mol. Sci., 2024, 25(7):4048, doi: 10.3390/ijms25074048, PMID:38612857

    IF: 4.9

9.2 Publications related to the subject of the dissertation

1. E Schwaner, Z Németh, PK Jani, E Kajdácsi, ML Debreczeni, Z Doleschall, J Dobó, P Gál, J Rigó, K András, T Hegedűs, L Cervenak

    Transcriptome analysis of inflammation-related gene expression in endothelial cells activated by complement MASP-1.

    Sci. Rep., 2017, 7(1):10462, doi: 10.1038/s41598-017-09058-8, PMID: 28874747

    IF: 4.112

2. ML Debreczeni, Z Németh, E Kajdácsi, E Schwaner, V Makó, A Masszi, Z Doleschall, J Rigó, FR Walter, MA Deli, G Pál, J Dobó, P Gál, L Cervenak

    MASP-1 Increases Endothelial Permeability.

    Front Immunol. 2019 May 3;10:991, doi: 10.3389/fimmu.2019.00991, PMID: 31130964

    IF: 5.085

3. ML Debreczeni, Z Németh, E Kajdácsi, H Farkas, L Cervenak

    Molecular Dambusters: What Is Behind Hyperpermeability in Bradykinin-Mediated Angioedema?

    Clin Rev Allergy Immunol. 2021 Mar 16:1–30. doi: 10.1007/s12016-021-08851-8, PMID: 33725263

    IF: 10.817

4. F Demeter, Z Németh, E Kajdácsi, G Bihari, J Dobó, P Gál, L Cervenak

   Detrimental synergistic effects of hypoxia and complement MASP-1 in endothelial cells as a model for atherosclerosis-related diseases.

   Sci. Rep. 2024 Jun 27, 14(1):14882, doi:10.1038/s41598-024-64479-6, PMID:38937560

   IF: 3.8

9.3 Publications independent of the subject of the dissertation

1. Z Baranyai, B Biri-Kovács, M Krátký, B Szeder, ML Debreczeni, J Budai, B Kovács , L Horváth, E Pári, Z Németh, L Cervenak, F Zsila, E Méhes, É Kiss, J Vinšová, S Bősze

   Cellular Internalization and Inhibition Capacity of New Anti-Glioma Peptide Conjugates: Physicochemical Characterization and Evaluation on Various Monolayer- and 3D-Spheroid-Based in Vitro Platforms.

   J Med Chem. 2021 Mar 25;64(6):2982-3005. doi: 10.1021/acs.jmedchem.0c01399. Epub 2021 Mar 15. PMID: 33719423

   IF: 8.039

10. ACKNOWLEDGEMENTS